Late Glacial-early holocene vegetation and environmental changes in the western Iberian Central System inferred from a key site: The Navamuño record, Béjar range (Spain)

José Antonio López-Sáez [a, *], Rosa M. Carrasco [b], Valentí Turu [b, c], Blanca Ruiz-Zapata [d], María José Gil-García [d], Reyes Luelmo-Lautenschlaeger [a], Sebastián Pérez-Díaz [e], Francisca Alba-Sánchez [f], Daniel Abel-Schaad [f], Xavier Ros [c], Javier Pedraza [g]

[a] Environmental Archaeology Research Group, Institute of History, CSIC, Albasanz 26-28, 28037, Madrid, Spain
[b] Department of Geological Engineering and Mining, University of Castilla-La Mancha, Avda. Carlos III s/n, 45071, Toledo, Spain
[c] Fundació Marcel Chevallier, Edifici Socio-Cultural de la Llacuna, AD500 Andorra la Vella, Andorra
[d] Department of Geology, Geography and Environment, University of Alcalá de Henares, 28871, Alcalá de Henares, Spain
[e] Department of Geography, Urban and Regional Planning, University of Cantabria, Avda. de los Castros s/n, 39005, Santander, Spain
[f] Department of Botany, University of Granada, 18071, Granada, Spain
[g] Department of Geodynamics, Stratigraphy and Paleontology, Complutense University, José Antonio Novais 12, 28040, Madrid, Spain

ARTICLE INFO

ABSTRACT

A new record from a long sediment core (S3) in Navamuño (1505 m asl, western Iberian Central System) provides the reconstruction of the vegetation history and environmental changes in the region between 15.6 and 10.6 ka cal BP, namely during the Late Glacial and the early Holocene, using a multiproxy analysis (pollen-based vegetation and climate reconstruction, sedimentary macrocharcoals, loss-on-ignition, magnetic susceptibility and X-ray fluorescence (XRF) measurements). The results are then compared with other sequences from the Iberian Central System and the whole Iberian Peninsula in order to better understand the past dynamics of the main forest constituents. The pollen record shows a shift from open pine forests ~15.6—14.7 ka cal BP (Oldest Dryas) to mixed open pine-birch woodlands ~14.7—14.0 ka cal BP (Bølling). Woodlands were succeeded by a steppe-like landscape until ~13.4 ka cal BP (Older Dryas), which was replaced again by high-mountain pine forests and riparian woodlands ~13.4 —12.6 ka cal BP (Allerød). A great development of cold steppe grasslands linked to the decline of birch woodlands is documented ~12.6—11.7 ka cal BP (Younger Dryas). The early Holocene (11.7—10.6 ka cal BP) was characterized by a progressive reforestation of the study area by pine and birch forests in the highlands and oak woods in the lowlands. Temperate tree taxa (*Carpinus betulus*, *Castanea sativa*, *Corylus avellana*, *Fraxinus*, *Juglans*, *Tilia*, and *Ulmus*) were also common but likely at lower elevations. Pollen of *Fagus sylvatica* was already recorded during the Late Glacial and the early Holocene. The marked increasing local fire activity during the warmer and wetter Allerød oscillation could be related to a rise in tree cover, supporting the climatically driven character of these fires. Nevertheless, the strong increase in fire activity during the Younger Dryas would probably be related to growing tree and shrub mortality, as well as to the wet/dry biphasic structure of this stadial. The standard "Modern Analogue Technique" has been also applied to the Navamuño sequence to provide quantitative climate estimations for the Late Glacial and the early Holocene periods. This record is one of the few continental archives that show the climatic trend between the Late Glacial and the early Holocene in central Iberia, agreeing with many other regional records from the Western Mediterranean.

© 2020 Elsevier Ltd. All rights reserved.

1. Introduction

Major climatic events during the late Pleistocene and the Holocene are well reconstructed and teleconnected in many parts of

the planet, especially in Western Europe, using a multiproxy approach (Watts et al., 1996; Allen and Huntley, 2000; Roberts et al., 2004; Fletcher et al., 2010; Moreno et al., 2014; Beaulieu et al., 2017; Sadori, 2018). However, in the Iberian Peninsula the data on such globally related climatic events are still very limited (Carrión et al., 2010; González-Sampériz et al., 2010). This problem is particularly acute in the Iberian Central System (ICS), where systematic palaeoecological works are still few. Although our knowledge is growing, we still lack a coherent vision on patterns of change and climatic conditions in the central Iberian highlands during late Quaternary glacial-interglacial cycling and the corresponding response of vegetation.

Late Glacial is characterized by a number of relatively short and rapid climatic changes. It is considered to be the transition period between the cold and dry Pleniglacial and the warm and wetter Holocene, dated to approximately 20−11.7 ka cal BP (González-Sampériz et al., 2010; Domínguez-Villar et al., 2013). Climatic oscillations during the late Pleistocene and the Holocene led to massive range shifts and shaped the genetic structure and diversity of biota (Comes and Kadereit, 1998). Both phylogeographic and palynological studies in Europe have confirmed the importance of the Iberian Peninsula as one of the main refuge areas for temperate flora during the Pleistocene glacial periods (Hewitt, 1999, 2000), as well as a source for the post-Pleistocene colonization of northern latitudes (Taberlet et al., 1998; Benito-Garzón et al., 2007, 2008). This situation has been substantially different for cold-adapted plant species, which survived the glacial stages in mountain ranges or in peripheral refugia (Schönswetter et al., 2005). These species probably extended their distribution ranges during cold periods and became isolated at high altitudes and/or latitudes during warm interglacial or interstadial periods (Vargas, 2003). By contrast, high-mountain trees are equally likely to have survived in refugia in the southern European peninsulas (Birks and Willis, 2008) as for example the ICS (López-Sáez and López-García, 1994; López-Sáez et al., 2019), which becomes a great natural laboratory for studying the resilience of certain species to climate variability and human impact, but also for understanding why other cold-adapted forest species have become extinct in these mountains.

Thanks to the confluence of diverse climates and a rich topography, the western ICS (western Gredos or Béjar range) harbors some of the highest plant diversity found throughout Iberia, with a vascular flora of more than 1400 species, 200 of which are endemic to the Iberian Peninsula and 12 to these mountains (Luceño and Vargas, 1991). However, Gredos' richness in endemism is lower than expected, likely related to the effect of cold Quaternary periods that were responsible for the extinction of numerous species (Vargas and García, 2008). The ICS is well characterized by Quaternary sediments of glacial-fluvial and lacustrine depositional environments, providing good natural archives for the multiproxy palaeoclimatic reconstructions of the late Pleistocene and early Holocene times (Pedraza, 1989, 1994; Domínguez-Villar et al., 2013). Nevertheless, apart from the western sector of the ICS (the Estrela range in Portugal), where the Late Glacial and the full Holocene are recorded in pollen sequences (van der Knaap and van Leeuwen, 1994, 1995, 1997), the rest of this mountain massif remains unpublished and no detailed high-resolution study of vegetation dynamics and climate evolution over the last 16 thousand years is known (Pontevedra et al., 2017). In order to compensate this lack of such records, several scientific projects have been aiming to systematically investigate key-sites from the western ICS, in order to establish an absolute chronology of the vegetation dynamics from the Late Glacial to the present day. Preliminary results reveal that the Gredos range appears to have acted as a refugium for coniferous and cold-adapted deciduous tree taxa (*Alnus glutinosa*, *Betula alba*, *Pinus nigra*, *P. sylvestris*), while

small areas with suitable microclimate may have acted as micro-refugia for warm demanding temperate taxa such as *Castanea sativa*, *Corylus avellana*, *Fraxinus excelsior*, *Juglans regia*, *Prunus lusitanica* and *Ulmus glabra* (López-Sáez, 1993; Rubiales et al., 2007; López-Sáez et al., 2010b, 2014, 2017, 2019). These records also shed light on the Holocene patterns of tree species expansion with several acknowledged forest stages: i) dominance of *Betula* in the western sector (Béjar range) and the prevalence of pinewoods eastwards (central-eastern Gredos range) at the onset of the post-glacial; ii) expansion of *Quercus* sp. during the mid-early late Holocene. However, pollen records have also shown that past vegetation dynamics was not uniform in the western ICS as initially believed; differences exist in the timing of the expansion of several forest taxa (Gil-Romera et al., 2010b; Morales-Molino et al., 2013; Abel-Schaad et al., 2014; López-Sáez et al., 2014, 2019).

Palynological studies into Late Glacial and early Holocene vegetation history in the Iberian Peninsula are now numerous (Carrión et al., 2010; González-Sampériz et al., 2010), however would greatly benefit from higher temporal resolution and better chronological control. To contribute in filling this gap, we performed a multiproxy palaeoenvironmental study of a Late Glacial to early Holocene sedimentary section from a key site in the Béjar range, western ICS, the Navamuño record. Our main objective is the reconstruction of the local environmental history including vegetation, fire and climate dynamics, in an attempt to identify mechanisms of past high-mountain ecosystem change during the Late Glacial and the early Holocene. It also sets to determine whether there are leads or lags in the establishment and expansion of main forest taxa, as compared to other regions from central Iberia.

2. Regional setting

The study area is located in the western part of the ICS (Fig. 1), the so-called Béjar range (western Gredos range). This range is a granite massif structured in the form of a block-mountain and limited by two large morphotectonic depressions. This network in combination with the E-W network, dominate the general morphostructure of the relief, the outline of the current drainage network and the main valleys of glacial origin (Carrasco, 1997). This NE-SW mountain range corresponds to an intraplate mountain structured in fault blocks and formed during the Alpine orogeny due to the tectonic reactivation of an ancient massif (the Hercynian or Variscan basement) (Casas-Sainz and de Vicente, 2009). The current morphostructure forms a piedmont stairway (piedmont-treppen), and the summit areas have altitudes of between 1700 and 2400 m asl (Pedraza, 1989, 1994). This morphology was a major factor in the development of glaciers in some of the summits of the Béjar range during the late Pleistocene. Its paleoglaciers are among the most important of the ICS, usually classified as valley cirque glaciers, although they have recently been reclassified as plateau glaciers (Carrasco et al., 2013). The predominant lithologies are granitoids; although migmatites, metasediments and quartzitic schists are also present (GEODE, 2004).

The Navamuño peat bog (40°19′16.80″N, 5°46′42.83″W) lies at 1505 m asl and was chosen because of its big catchment and its remote position far from the valleys in the north and south of the Béjar range which are more strongly impacted by human activities. It corresponds to a *nava*-type bucket located at the head of the Cuerpo de Hombre valley that is confined laterally by both glacial (moraines) and morpho-structural elements (escarpments) (Fig. 1) (Carrasco et al., 2015a, 2015b). The Cuerpo de Hombre paleoglacier occupies the upper sector of the Cuerpo de Hombre river basin, located on the northwest slope of the Béjar range. The peat bog has an area of ca. 14 ha with a sediment thickness greater than 20 m (Carrasco et al., 2018; Turu et al., 2018) and is therefore likely to
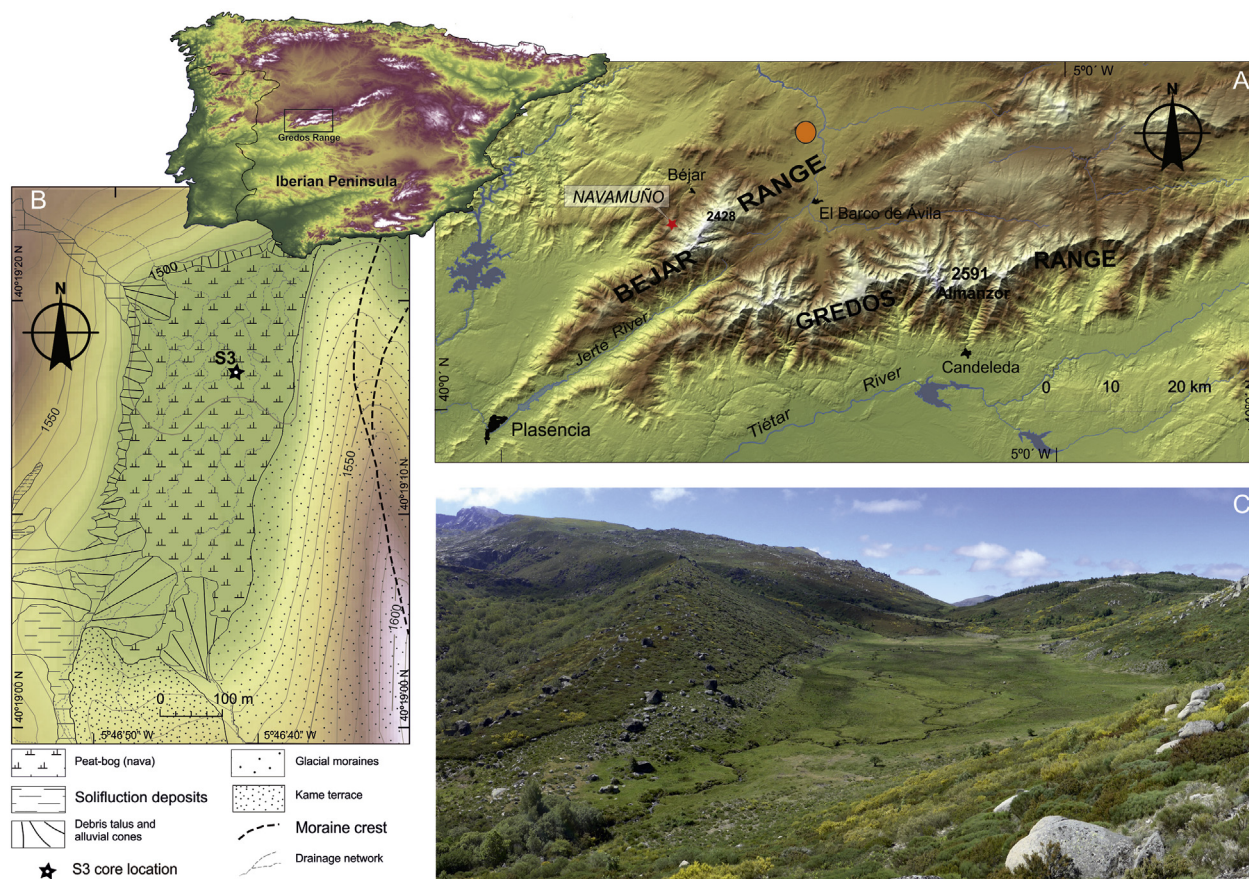
Fig. 1. Location of the Navamuño peat bog (A); geomorphological scheme of the Navamuño depression or *nava* where the S3 core is located (B); general view of the peat bog and *nava* from the southwest (C). The orange circle indicates the location of the Upper Palaeolithic site mentioned in the text. (For interpretation of the references to color in this figure legend, the reader is referred to the Web version of this article.)

record both local and regional vegetation changes in the past. During the last glacial period, in the Cuerpo de Hombre valley, one of the largest glacial tongues (~6 km^2) in central Iberia developed, which formed part of the glacial plateau of the Béjar range (Carrasco et al., 2013). The chronological data obtained in the boulders of moraines by ^{10}Be indicate an age of ~25.0 ka cal BP for the maximum ice extent of Cuerpo de Hombre paleoglacier (Carrasco et al., 2015a). This chronology coincides with date obtained for other paleoglaciers in the ICS, but is slightly more modern than the regional chronology estimated as most likely for the maximum ice extent in these areas (Palacios et al., 2011; Domínguez-Villar et al., 2013). Subsequent to reaching the maximum extent, the glacier had a first retreat (minimum age ~20.6 ka cal BP), followed by another stage of expansion or re-advance, after which it stabilised until the start of the deglaciation stage ~17.8 ka cal BP (Pedraza et al., 2013).

From a phytogeographical point of view, the peat bog is located in the Bejaran-Gredensean sector of the Carpetan-Leonese sub-province of the Mediterranean West Iberian province of the Mediterranean region (Rivas-Martínez, 2007). The local vegetation type is assigned to the Caricetum echinato-nigrae and Calluno vulgaris-Sphagnetum capillifolii plant communities (Sardinero, 2004). The peat bog vegetation is mainly composed of *Carex echinata*, *C. nigra*, *C. demissa*, *Sphagnum* sp., *Drosera rotundifolia*, *Calluna vulgaris*, *Potentilla erecta*, *Agrostis canina*, *Nardus stricta*, *Viola palustris*, *Eleocharis quinqueflora*, *Epilobium palustre*, and *Gentiana boryi*. The specific vegetation stage for this altitude (1505 m asl) is typically characterized by the Cytiso oromediterranei-Genistetum

cinerascentis plant community and for higher altitudes (above 1750 m asl) by the Cytiso oromediterranei-Echinospartetum pulveniformis plant community (Sardinero, 2004). The first corresponds to broom communities from the upper supramediterranean humid belt dominated by *Cytisus oromediterraneus*, *C. scoparius*, *Genista cinerascens*, *Festuca elegans* subsp. *merinoi*, *F. gredensis*, *Pteridium aquilinum*, and, to a minor extent, *Erica australis* subsp. *aragonensis*. These broom communities represent serial stages of the *Quercus pyrenaica* forests that disappeared in the study area due to the systematic burning that the territory has suffered in the last two centuries. The second one represents orotemperate submediterranean (orosubmediterranean) hyperhumid broom communities from the oromediterranean belt dominated by *Cytisus oromediterraneus*, *Echinospartum ibericum* subsp. *pulvifinormis* and *Juniperus communis* subsp. *alpina*. At lower altitudes (900−1300 m asl) subhumid supramediterranean oak forests of *Quercus pyrenaica* (Festuco merinoi-Quercetum pyrenaicae community) dominate the landscape. Planted *Pinus sylvestris* woods grow within them. *Castanea sativa* and *Juglans regia* grow up to an elevation of 1000 m asl on sunny southern slopes. These forests connect at lower altitudes to the south with the upper mesomediterranean oak forests (Arbuto unedonis-Quercetum pyrenaicae), characterized by the presence of *Arbutus unedo* (López-Sáez et al., 2015), and lower mesomediterranean evergreen oak woodlands (Pyro bourgaeanae-Quercetum rotundifoliae community) dominated by *Quercus ilex* subsp. *rotundifolia*. *Alnus glutinosa*, *Salix atrocinerea* and *Sorbus aucuparia* make mainly up the riparian woodlands.

The climate is of a Mediterranean type, with a summer drought

period and more intense rainfall in autumn and winter, although it is influenced by Atlantic depressions from the southwest and the Azores anticyclone. Average annual rainfall on the Béjar mountains ranges between 800 and 1000 mm, reaching about 2000 mm at the summits, while temperature varies between −4 and 3 °C during winter and 22 and 32 °C during summer; mean annual temperature is 9.5 °C (Sardinero, 2004; Fick and Hijmans, 2017).

3. Material and methods

3.1. Core sampling, lithology and chronology

A 1586 cm-long sediment core (S3) was recovered from the central-north area of the Navamuño depression in 2015 (Fig. 1) using a modified squared-rod piston corer. Below these levels a layer rich in kaolinite (1600-1586 cm) was documented, but is not considered in this study. Core description and sampling procedures are described in Turu et al. (2018). At the Department of Geodynamics, Stratigraphy and Paleontology, Complutense University, Spain the core was split lengthwise, photographed and described lithologically (Table 1) and then stored in darkness at 4 °C. Two palynological hiatuses were documented at 593-567 cm (~8.9–8.4 ka cal BP) and 706-605 cm (~10.6–9.2 ka cal BP) coinciding with a lithostratigraphy of coarse sand with gravels and pebbles. Probably, such sedimentological characteristics provoked abrasive processes that destroyed the sporopollinic content (Carrión et al., 2009). This study uses the core section from 1586 to 707 cm depth below the lower hiatus, which corresponds only to the Late Glacial-early Holocene sediments, whose stratigraphy is represented in Fig. 2. Five organic sediment samples were selected for ^{14}C dating in the accelerator mass spectrometry (AMS) laboratory of Beta Analytic Inc. (Miami, USA), and their radiocarbon ages were calibrated to calendar ages using CALIB 7.1 software (Table 2) with the INTCAL13 curve (Reimer et al., 2013). An age-depth model was produced by using Clam 2.2 software (Blaauw, 2010). The best fit was obtained applying a smoothing spline (0.2 smooth) to the available radiocarbon dates. Confidence intervals of the calibrations and the age-depth model were calculated at 95% (2σ) with 10,000 iterations (Fig. 2).

3.2. Geochemical analysis

Geochemical elemental analysis of the S3 core was conducted at the CORELAB laboratory of the University of Barcelona, Spain. The core was run through an *Avaatech* XRF core-scanner at contiguous 1-cm intervals, and the final analysis focused on the ratios between aluminium (Al) and titanium (Ti) on the one hand and manganese (Mn) and iron (Fe) on the other. The Al/Ti record is interpreted as a measure of density differences in siliciclastic materials derived from fluvial and aeolian sources in lacustrine sediments (Höobig et al., 2012) in regions which are mainly characterized by terrigenous components in the palaeolake system through time (López et al., 2006; Schröder et al., 2018). Therefore, Al and Ti can be used as efficient indicators of transportation energy changes by their different elementary gravity. Ti is a detrital sediment indicator in our record because it is only produced allogenically through the physical erosion of Ti-bearing rocks (Cohen, 2003), and mineral containing Ti are not sensitive to dissolution (Demory et al., 2005). Mn and Fe are sensitive to geochemical changes in the depositional environment so that the Mn/Fe ratio is often used as a proxy for paleo-redox conditions (Koinig et al., 2003). Mn is highly insoluble in the water column in oxygenated conditions and consequently elevated Mn/Fe ratio depicts an oxygen-rich environment, whereas low Mn/Fe ratios reflect more oxygen-depleted conditions at the water/sediment interface.

3.3. Loss-on-ignition, magnetic susceptibility and sedimentary macrocharcoal analysis

The organic matter content of the sediment (1 cm^3) was determined for consecutive 5-cm sub-samples by loss-on-ignition (LOI) following sequential heating at 550 °C for 4 h and 950 °C for 1 h (Heiri et al., 2001). LOI is expressed as a percentage of weight loss in dried sediment. Before other analyses were made, magnetic susceptibility (MS) was measured at a resolution of 6 ± 1 cm using a pocket-sized Gf Instrument SM-20 magnetic susceptibility meter to reveal environmental changes recorded in the sediment. Measurements were reported in SI units. The sediment macrocharcoal count was performed with the sieving method (Carcaillet et al., 2001) with a 150 μm mesh size in order to reconstruct local fire history, calculating the area using an ocular micrometer with a graticule of 10 × 10 squares each with an area of 0.0625 mm^2. To minimize the effects of the different sample densities, the choice was made to work with weight (~1 g) rather than volume (Carcaillet et al., 2007). The samples were weighed and then heated at 70 °C for 90 m, adding two tablets of a defloculant solution of KOH and 20 ml of NaClH (15%) to each sample to eliminate organic matter and respectively bleach the samples (Finsinger et al., 2014). Charcoal concentration was expressed in mm^2/g.

3.4. Pollen analysis

Pollen analysis was carried out on 115 sub-samples of 1 cm^3 volume along the lower 879 cm of the core (1586-707 cm) at ~5 cm intervals using the standard acid-alkali method of Moore et al. (1991). The core had a particularly good resolution for the Late Glacial-early Holocene, ~15.6 to ~10.6 ka cal BP, providing nearly decadal resolution (5.63 yr/cm). Palynomorphs were identified at 400x and 1000x magnification to the lowest taxonomic level possible. Identifications were based on the European and North African Atlas (Reille, 1999), and the pollen reference collection at the Institute of History (CSIC-Madrid). Oleaceae pollen types were discriminated according to Renault-Miskovsky et al. (1976); *Pinus pinaster* and *Erica australis* pollen differentiation followed Mateus (1989), Carrión et al. (2000) and López-Sáez et al. (2010b). *Plantago coronopus*-type is named after Ubera et al. (1988) and includes *Plantago maritima*, *Plantago alpina* and *Plantago subulata*. Non-pollen palynomorphs (NPPs) were identified in parallel to pollen counting using available literature (van Geel, 2001; Carrión and Navarro, 2002; Cugny et al., 2010). NPP nomenclature follows current common rules (Miola, 2012) with the abbreviations HdV-xxx (Hugo-de-Vries Laboratory, University of Amsterdam, Amsterdam, The Netherlands), for the according laboratory that described them first. Pollen counts of up to 400 grains total land pollen (trees, shrubs, herbs) per sample were identified and counted. Pollen of aquatic or wetland plants as well as spores and non-pollen
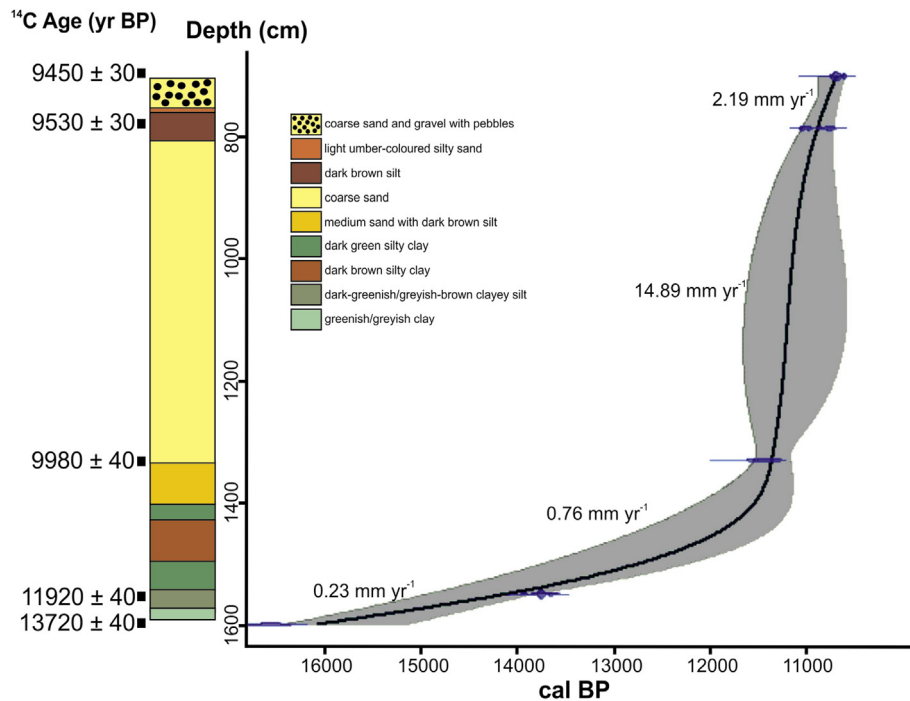
Table 1
Simplified stratigraphic description of the Navamuño sequence (S3 core).

Depth (cm)	Stratigraphic description
707−753	Coarse sand and gravels with pebbles
753−758	Light umber-coloured silty sand
758−803	Dark brown silt
803−1330	Coarse sand
1330−1400	Medium sand with dark brown silt
1400−1420	Dark green silty clay
1420−1495	Dark brown silty clay
1495−1542	Dark green silty clay
1542−1576	Dark-greenish/greyish-brown clayey silt
1576−1586	Greenish/greyish clay

Fig. 2. Lithostratigraphy and age-depth relations for the Navamuño sequence. Samples providing the AMS and calibrated ^{14}C ages (blue points) are listed in Table 2. The model (smooth spline 0.2, black line) takes into account 2σ-confidence range of calibrated ages (grey areas). Sediment accumulation rates (SARs in mm yr^{-1}) are shown between individual radiocarbon ages. (For interpretation of the references to color in this figure legend, the reader is referred to the Web version of this article.)

Table 2
AMS and calibrated^{14}C ages for the S3 core sequence from the western Gredos range, Iberian Central System, Spain.

Lab code	Depth (cm)	Material dated	^{14}C Age BP	Calibrated range (cal BP)	Median probability (cal BP)
β-410,000	700	Cyperaceae seeds	9450 ± 30	10,754–10587	10,686
β-410,001	785	Cyperaceae seeds	9530 ± 30	11,072–10707	10,868
β-410,003	1330	Bulk	9980 ± 40	11,619–11264	11,426
β-410,004	1550	Cyperaceae seeds	11,920 ± 40	13,942–13568	13,744
β-412,870	1600	Bulk	13,720 ± 40	16,800–16339	16,561

palynomorphs (NPPs) were excluded from the pollen sum and their percentages were calculated relative to the total land pollen sum of all terrestrial taxa taken as 100%. Interpretation of the pollen percentage data was based on a comparison with modern pollen data from the ICS (López-Sáez et al., 2010a, 2013, 2015). To establish the zonation of the pollen sequence, we tested several divisive and agglomerative methods with the program IBM SPSS Statistics 21. Based on the ecological meaning of the obtained zones, four local pollen assemblage zones (LPAZ-1 to LPAZ-4) were constructed on the basis of agglomerative constrained cluster analysis of incremental sum of squares (Coniss) with square root transformed percentage data (Grimm, 1987). The number of statistically significant zones was determined by using the broken-stick model (Bennett, 1996). A total of 87 pollen, spore, and non-pollen palynomorph types were identified. The results of the identification and counting are presented as percentage diagrams (Figs. 3–5). The pollen diagrams have been plotted against age, using TGview (Grimm, 2004). The terms 'local' (0–20 m), 'extra-local' (20 m-2 km), and 'regional' (>2 km) used in the text refer to different pollen source areas according to Prentice (1985).

3.5. Pollen-based palaeoclimate reconstruction

Quantitative estimates of mean annual temperature (Tann) and total annual precipitation (Pann) during the Late Glacial and the early Holocene are inferred from Navamuño pollen data with the Modern Analogue Technique (MAT) (Guiot, 1990; Peyron et al., 2005). In the MAT method, the similarity between each fossil sample and modern pollen assemblage is evaluated by a squared chord distance (Birks et al., 2010). Estimates of past climatic parameters are obtained by taking a weighted average of the values for all selected best modern analogues, where the weights used are the inverse of the chord distance. To reduce uncertainties, we have used only the modern pollen rain database of the Iberian Peninsula (Davis et al., 2013). To improve the climate reconstruction, in particular to reduce the potential effect of spatial autocorrelation (Telford and Birks, 2005), we have updated the modern pollen dataset using 1147 surface samples distributed along a large precipitation and temperature gradient and a wide variety of ecosystems throughout the Iberian Peninsula. The MAT model was developed using C2 1.7.4 software (Juggins, 2007) and the World-Clim version 2 (Fick and Hijmans, 2017) for climate variables (~1 km^2 of spatial resolution). We chose the model with the smallest root mean squared error of prediction (RMSEP) value and largest high coefficient of determination between predicted and observed values (R^2). Two-component models for reconstruction were selected for Tann ($R^2 = 0.86$, RMSEP = 1.19) and Pann ($R^2 = 0.79$, RMSEP = 94.78). The current average climatic values obtained for the study area via Worldclim database were Tann (8.8 °C) and Pann (726 mm), respectively. The latter are taken as
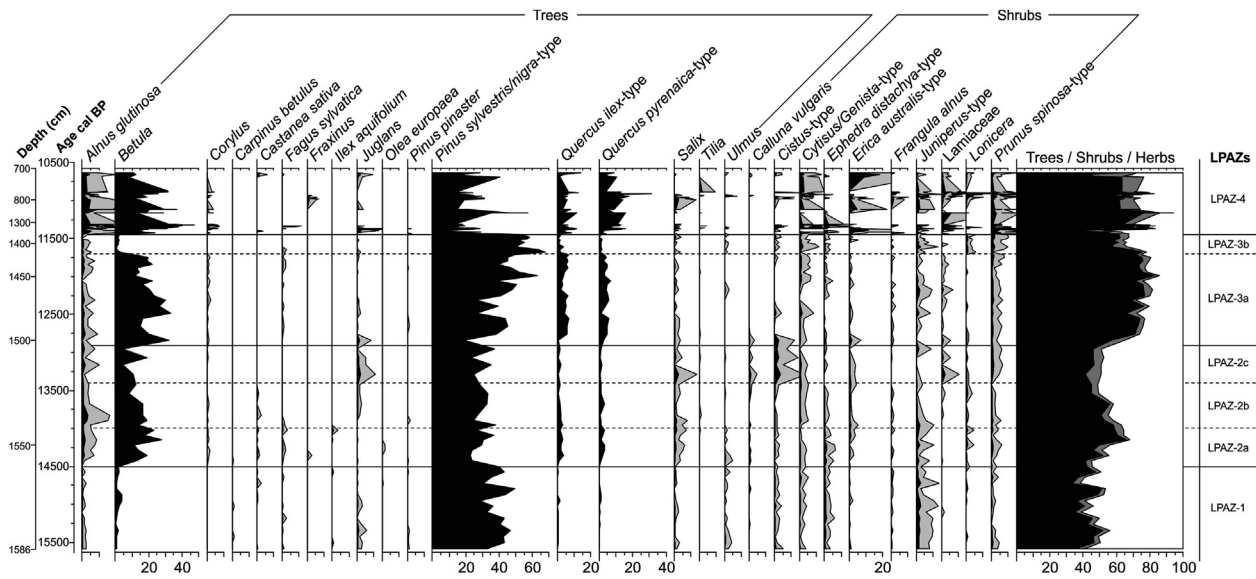
Fig. 3. Percentage pollen diagram of the S3 core (woodland vegetation) plotted against age (cal BP). The black silhouettes show the percentage curves of the taxa, the grey silhouettes show the ×5 exaggeration curves.
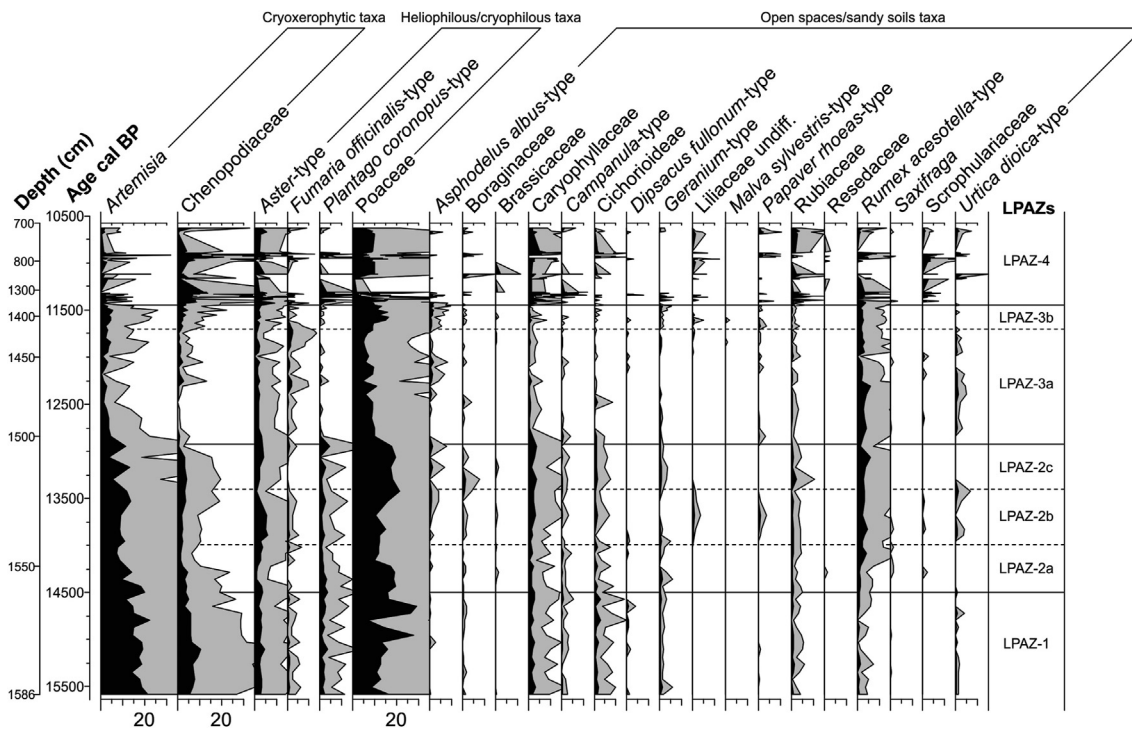

Fig. 4. Percentage pollen diagram of the S3 core (herbs) plotted against age (cal BP). The black silhouettes show the percentage curves of the taxa, the grey silhouettes show the ×5 exaggeration curves.

reference data for the estimated climatic values (Pann and Tann) throughout the pollen sequence.

4. Results

The sedimentary profile of the Navamuño sequence is certainly complex (Fig. 2), as it has different levels of clay, silt, clayey silt, silty clay, silty sand as well as other of sand of different texture including some with gravel and pebbles (753-707 cm). Between 1330 and

803 cm the sedimentary record shows a remarkable layer of almost 5 m characterized by containing almost exclusively coarse sands. A simplified stratigraphy of the sequence (1586-707 cm cm) is presented in Table 1 and also given in Fig. 2. S3 core spans the last 15.6 ka cal BP years (Table 2). All radiocarbon dates appear in stratigraphical order. The series of five AMS dates shows a consistent age-depth model (Fig. 2), which possibly indicates that there is no presence of hiatus. The core shows a low sedimentation rate (~0.23−0.76 mm yr^{-1}) between the bottom of the core (1586 cm)
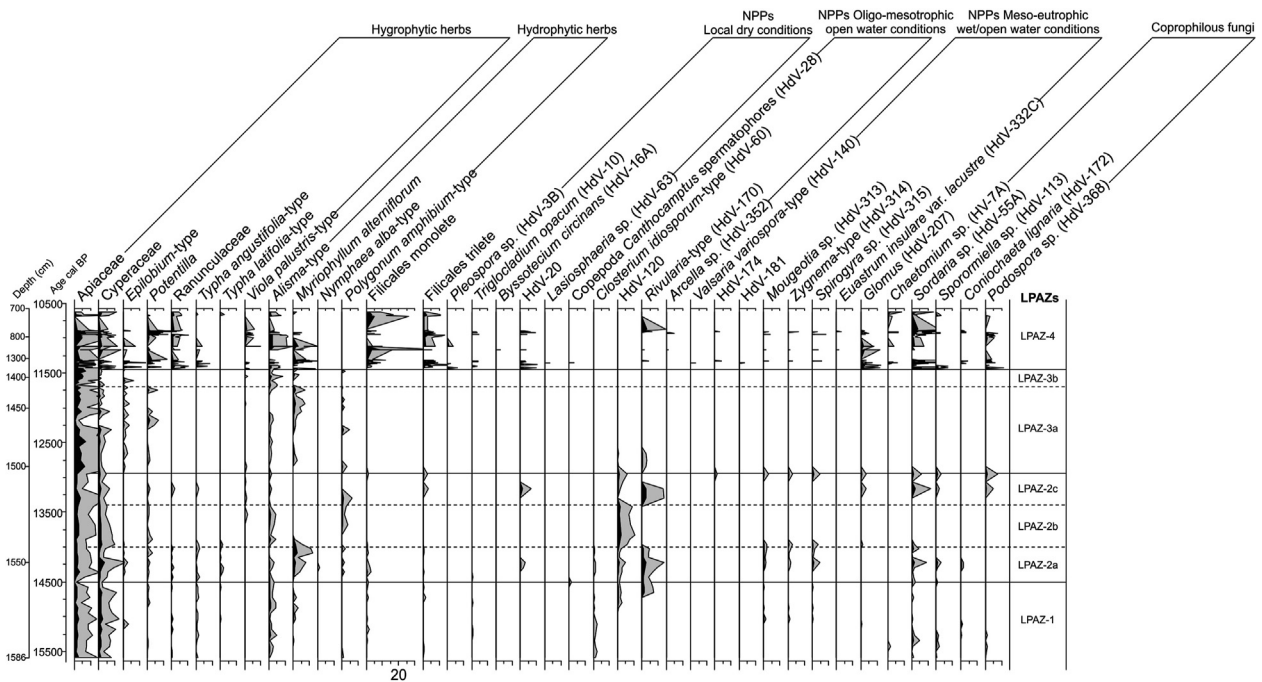
Fig. 5. Percentage pollen diagram of the S3 core (hydro-hygrophytic taxa, ferns and non-pollen palynomorphs) plotted against age (cal BP). The black silhouettes show the percentage curves of the taxa, the grey silhouettes show the ×5 exaggeration curves.

and 1330 cm depth, and higher values (~14.89 mm yr^{-1}) between 1330 and 785 cm, and, finally sedimentation rate stabilizes (~2.19 mm yr^{-1}) between 785 and 707 cm (Fig. 2).

The size of the sedimentary basin is ~14 ha therefore the pollen assemblages are representative of vegetation composition of a relatively large kilometers radius, i.e. both locally and regionally (Sugita, 1994; Gaillard et al., 2008). For the Navamuño sequence, 115 pollen spectra were analyzed and 85 taxa were identified. To facilitate description and interpretation of the pollen diagrams with respect to vegetational changes, 4 Local Pollen Assemblage Zones (LPAZs 1–4) were established, although LPAZ-2 and LPAZ-3 contain 3 and 2 sub-zones each, respectively (Table 3; Figs. 3–5). The main vegetation development is highlighted in Table 3.

A synthetic diagram including selected ecological groups, macrocharcoal abundance, LOI, MS, Al/Ti and Mn/Fe ratios, the reconstructed values of annual average temperature (Tann) and total annual precipitation (Pann) using the MAT technique, and δ^{18}O record from NGRIP record (Rasmussen et al., 2008) plotted against age (cal BP) is shown in Fig. 6. Macrocharcoal particles are practically absent ~15.6–12.9 ka cal BP (1586-1500 cm), except ~14.3–13.8 ka cal BP (1552-1538 cm), where macrocharcoal area reaches 0.2–0.3 mm^2/g (Fig. 6). The period ~12.9–11.3 ka cal BP is characterized by rapid accumulation of macrocharcoal, with maxima values (1.6–2.2 mm^2/g) between 11.5 and 11.4 ka cal BP. Subsequently, a new maximum is documented ~10.9 ka cal BP (0.8 mm^2/g). Total organic matter content in the Navamuño S3 core, as approximated by the LOI (Fig. 6), shows great variability throughout the sequence. Although their values are not very high there are four characteristic phases with a higher average (>20%) content: 779 cm, 1340 cm, 1379 cm, and 1458 cm. Two high positive MS peaks (>0.6 × 10^3 SI units) coincide with sand layers (Table 1) ~11.37 ka cal BP (1350 cm) and 11.05 ka cal BP (839 cm), respectively (Fig. 6).

5. Discussion and regional comparison

The Navamuño record starts ~15.6 ka cal BP and spans the entire Late Glacial and early Holocene periods until ~10.6 ka cal BP. The pollen, macrocharcoal, LOI, MS and geochemical records from Navamuño indicate that major changes occurred in the lacustrine landscape, involving the forest/shrub cover and the herbaceous vegetation, as well as the submerged and floating plant coenoses. These changes are discussed in relation to: i) the regional development of vegetation in the Iberian Peninsula; ii) the evolution of the lacustrine environment; iii) the main climate fluctuations recorded by the proxy NGRIP δ^{18}O curve at the late Pleistocene-early Holocene transition (Fig. 6).

5.1. Oldest Dryas stadial (~15.6–14.7 ka cal BP)

The basal pollen zone (LPAZ-1; 1586-1557 cm; ~15.6–14.5 ka cal BP) shows the highest percentages of herbs (50–62%), mainly represented by cryoxerophytic taxa (Artemisia, Chenopodiaceae, Ephedra distachya) and heliophilous/cryophilous herbs (Poaceae, Aster, Fumaria officinalis, Plantago coronopus), probably indicating cold and dry conditions (Figs. 3, 4 and 6). This pollen assemblage points to a great development of open vegetation on the surrounding landscape. Other herb pollen types (Fig. 4) having limited dispersal capacities and possibly derived from plants growing near the S3 core include plants typical of open, sandy soils (Caryophyllaceae, Campanula, Cichorioideae, Geranium, Rubiaceae, Rumex acetosella). The arboreal pollen sum (33–52%) is mainly made up of abundant pollen-producing cold-adapted tree taxa such as Pinus sylvestris/nigra, Betula, Alnus and Salix, indicating the presence of open pine forests and sparse riparian woodlands in the proximity of the Navamuño depression (Figs. 3 and 6). Juniperus and Cytisus/Genista are continuously present at values ~1%. Both pollen taxa produce large quantities of pollen, but low amounts of pollen are usually found in mountain fossil records (Markgraf, 1980). Similar peaks in Juniperus and Cytisus/Genista pollen are

Table 3

Summary of the pollen stratigraphy, chronology and vegetation history of Navamuño peat bog (see Figs. 3–6 for pollen diagrams).

LPAZs	Depth (cm)	Age ka cal BP	Description	Inferred local upland vegetation
LPAZ-1	1586 −1557	15.6 −14.5	This zone is marked by the presence of cold-adapted trees. Among them, *Pinus sylvestris/nigra* (28−49%) is the dominant taxon. There is also a continuous curve of *Alnus, Betula* and *Salix* (<4%). *Carpinus betulus* percentages reach 0.3% and *Fagus* 0.5%. Temperate taxa (*Castanea, Juglans, Ulmus*) are also present with very low percentages (<1%). *Juniperus* was found in amounts higher than 1%, while *Cytisus/Echinospartum* reaches ~1%. Cryoxerophytic herbs (*Artemisia* 11−22%, Chenopodiaceae 3−10%) and heliophilous/cryophilous herbs (Poaceae 7 −29%, *Aster* 2−5%) are well represented. Scant presence of local hydro/hygrophytic taxa (<3%). In the upper part of the zone (~14.7−14.5 ka cal BP) there is an increase in NPPs indicators of oligotrophic open water conditions (HdV-120, HdV-170) suggesting an increase in rainfall, while the lower part is characterized by the presence of HdV-60 suggesting oligo-mesothropic wet open water conditions. Relatively low values (<1%) of coprophilous fungi (HdV-55A, HdV-113, HdV-172, and HdV-368) were present during this zone.	Open forest dominated by *Pinus sylvestris/nigra* with broom communities and crawling junipers. Presence of riparian woodlands (*Alnus, Betula, Salix*). Establishment of *Carpinus betulus* and *Fagus sylvatica*. The abundance of cryophilous and xerophytic herbs suggests cold and dry conditions, while since 14.7 ka cal BP rainfall seems to increase according to the percentage increase of NPPs indicators of oligotrophic open water conditions. The low percentage values of coprophilous fungi would indicate the presence of wild animals in the environment of the Navamuño depression. Presence of an amictic lake with glaciolacustrine depositional characteristics and oligo-mesothropic open cold water conditions.
LPAZ-2a	1557 −1542	14.5 −14.0	One of the major characteristics of this sub-zone is the decrease of *Pinus sylvestris/nigra* (23−38%), with the replacement mainly by *Betula* (11 −23%), *Alnus* (~2%) and *Salix*. Pollen of *Corylus, Castanea, Fagus, Fraxinus, Ilex Juglans, Tilia, Ulmus* and *Olea* was also present. *Carpinus betulus* disappears, while both evergreen and deciduous *Quercus* increase. *Juniperus* and *Cytisus/Genista* remain at low percentages and *Lonicera* (1%) slightly increases. This sub-zone comprises a phase with a marked decline of cryoxerophytic taxa (*Artemisia* 7−14%, Chenopodiaceae 1−4%). Heliophilous/cryophilous herbs increase at the beginning of the sub-zone and decrease drastically afterwards (Poaceae 20 to 10%, *Plantago coronopus* 3 to 1%). Hydro-hygrophytic taxa (*Myriophyllum* ~3%) and NPPs indicators of oligotrophic open water conditions (HdV-120, HdV-170−3%), as well as Zygnemataceae spores (HdV-313, HdV-314, HdV-315) slightly increase.	Open mixed woodland dominated by *Pinus sylvestris/nigra* and *Betula*. Temperate taxa were also common. The increase of hydro-hygrophytic herbs and meso-oligothropic open water indicator NPPs and the decline of cryoxerophytic elements suggest an increase in precipitation and a higher water table. Presence of a palaeolake with oligo-mesotrophic open water conditions.
LPAZ-2b	1542 −1520	14.0 −13.4	This sub-zone has a number of characteristics including: a) a temporary decrease of *Betula* (below 20%), *Salix*, evergreen *Quercus* and *Juniperus*; b) a slight increase of *Pinus sylvestris/nigra* (up to 25%), *Alnus, Castanea, Juglans* and *Cytisus/Genista*; c) *Fagus sylvatica, Fraxinus* and *Ilex* disappear; d) a notably increase of cryoxerophytic taxa (*Artemisia* up to 10%) and heliophilous/cryophilous herbs (mainly represented by Poaceae, *Aster* and *Fumaria officinalis*); e) disappearance of certain hydro-hygrophytic taxa (*Epilobium, Myriophyllum, Nymphaea*, Ranunculaceae, *Typha* sp.) but others increase (*Alisma, Polygonum amphibium*). Throughout the sub-zone, there are continuous occurrences of HdV-120 while HdV-60, HdV-170, HdV-313, HdV-314, HdV-315, while coprophilous fungi (HdV-55A, HdV-113, and HdV-172) disappear.	Open woodland dominated by *Pinus sylvestris/nigra* with broom communities and crawling junipers. *Betula* and *Alnus* were also common within the riparian woodlands. Some temperate taxa continue to be common. Cold and dry conditions are suggested by the increase of cryoxerophytic and heliophilous/cryophilous herbs and the decline of most hydro-hygrophytic taxa. The presence of HdV-120 suggests a lacustrine deposit.
LPAZ-2c	1520 −1500	13.4 −12.9	There is a marked increase in *Betula* (32%), *Juglans, Salix, Cistus* and Poaceae. The percentages of *Pinus sylvestris/nigra* fluctuate between 19 and 37%, while those of *Artemisia* fluctuate between 4 and 13%. A significant characteristic is the general decline and even disappearance of many hygrophytic and hydrophytic herbs, such as *Alisma, Polygonum amphibium*, Cyperaceae, etc, especially at the end of the sub-zone. The regular occurrence of HdV-170 in the first half of the sub-zone, suggests oligrotrophic open water conditions, while the predominance of HdV-120, HdV-174, HdV-313, HdV-314 and HdV-315 in the second half of the sub-zone suggests a change in trophic conditions towards meso-euthropic wet/open water conditions. Increasing values of coprophilous fungi (HdV-55A, HdV-113, and HdV-368) were present during this sub-zone. The presence of *Glomus* would be indicative of erosive processes.	Open mixed woodland dominated by *Pinus sylvestris/nigra* and *Betula* with broom communities and crawling junipers. Regional development of temperate and more thermal elements such as walnut and rockrose. Presence of a palaeolake with oligotrophic open water conditions at the bottom and meso-euthropic ones at the top.
LPAZ-3a	1500 −1420	12.9 −11.7	The pollen spectra are dominated by *Pinus sylvestris/nigra* (26−63%) and *Betula* (11−33%) at high altitudes although following antagonistic curves, and *Quercus* species, *Corylus* and *Fagus* at lower altitudes. *Juniperus* and *Cytisus/Genista* pollen occur regularly. The cryoxerophytic taxa (*Artemisia*, Chenopodiaceae, *Ephedra distachya*) and the heliophilous/cryophilous herbs (Poaceae, *Aster, Plantago coronopus*) show a continuous curve with alternating maximum and minimum percentages, as well as hydro-hygrophytic ones. Within NPPs, only HdV-120 and HdV-170 are present at the bottom of the zone.	~12.9−12.6 ka cal BP: Open woodland dominated by *Pinus sylvestris/nigra* with broom communities and crawling junipers. Increased values of hydro-hygrophytic herbs and the presence of meso-oligotrophic open water indicator NPPs, as well as the decline of cryoxerophytic taxa suggest an increase in precipitation. Presence of a palaeolake with oligo-mesotrophic open water conditions. Reappearance of beech. Development of oak woodlands at lower altitudes. ~12.6−11.7 ka cal BP: Landscape dominated by open high-mountain pine forests and cold steppe grasslands. Strong decline of birch woodlands. Develop of hygrophytic elements in a marshy environment. NPPs are not recorded.
LPAZ-3b	1420 −1375	11.7 −11.45	This zone is characterized by the increase of *Pinus sylvestris/nigra* (>50%), *Cytisus/Genista* and *Juniperus*, and by the notably reduction of *Betula* (<3%), *Corylus, Fagus sylvatica* and both evergreen and deciduous *Quercus*. The regular occurrence of cryoxerophytic (*Artemisia*, Chenopodiaceae, *Ephedra distachya*) and heliophilous/cryophilous taxa (Poaceae, *Aster, Plantago coronopus*), as well as the general decline of hydro-hygrophytic herbs suggests dry conditions. However, the presence	Forest dominated by *Pinus sylvestris/nigra* with broom communities and crawling junipers. Open areas dominated by steppe-like vegetation. The Navamuño depression was occupied by a floodplain. NPPs are not recorded.

Table 3 (*continued*)

LPAZs	Depth (cm)	Age ka cal BP	Description	Inferred local upland vegetation
			of *Alisma*, Cyperaceae, *Epilobium* and *Myriophyllum alterniflorum* suggests the local existence of a floodplain. Higher *Asphodelus albus* values are indicative of a higher frequency of fires.	
LPAZ-4	1375 −707	11.45 −10.6	This zone is characterized by higher percentage values of *Betula* (>20%) and *Alnus* and a declining trend of *Pinus sylvestris/nigra*, although pine and birch generally follow antagonistic trends. High-altitude shrublands are dominated by *Cytisus/Genista* and *Juniperus*, as well as by *Erica australis* from 11.3 ka cal BP. *Fagus sylvatica* is only present at the bottom, while *Juglans* has a more or less continuous curve. Evergreen and deciduous oak woodlands develop at lower altitudes. The cryoxerophytic taxa (*Artemisia*, Chenopodiaceae, *Ephedra distachya*) and the heliophilous/cryophilous herbs (Poaceae, *Aster*, *Plantago coronopus*) show higher values at the bottom of the zone, while most hydro-hygrophytic taxa (Cyperaceae, *Potentilla*, *Viola palustris*, *Alisma*) increase their percentages at the top of the zone. Within NPPs, local dry conditions indicators (HdV-3B, HdV-10, HdV-16A, HdV-20, and HdV-63) are more abundant at the bottom of the zone, while oligo-mesotrophic open water conditions indicators (HdV-170) predominate at the top. Progressively higher values of *Quercus pyrenaica* and *Q. ilex*.	~11.45−11.3 ka cal BP: Open mixed woodland dominated by *Betula* and *Pinus sylvestris/nigra* with broom communities, crawling junipers and heaths. Regional development of temperate elements such as beech and walnut. The abundance of cryophilous and xerophytic taxa, as well as NPPs indicators of local dry conditions, suggests a cold, dry climate. ~11.3−10.6 ka cal BP: Open mixed woodland dominated by *Quercus pyrenaica*, *Betula* and *Pinus sylvestris/nigra* with broom communities, crawling junipers and heaths. *Fagus sylvatica* disappears. Lower cryophilous and xerophytic taxa values and higher hydro-hygrophytic taxa values suggest warmer and wetter conditions. Presence of an alluvial plain with oligo-mesotrophic open water conditions.

also seen in other records from central and northern Iberia during this period (van der Knaap and van Leeuwen, 1997; González-Sampériz et al., 2006, 2010), as well as from central and southern Italy (Watts et al., 1996; Drescher-Schneider et al., 2007; Sadori, 2018), suggesting the development of high-mountain broom communities and crawling junipers within the open pine woodlands (López-Sáez et al., 2013; Broothaerts et al., 2018). Low percentages of temperate taxa (*Carpinus betulus*, *Castanea*, *Juglans*, and *Ulmus*) suggest that small populations of these trees were established regionally, probably in the lowlands in particular humid shelters of the Gredos range or confined to river banks (López-Sáez, 1993; López-Sáez and López-García, 1994; Abel-Schaad et al., 2014; López-Sáez et al., 2017). *Fagus sylvatica* is also recorded sporadically with very low percentages (<0.2%; Fig. 3) suggesting and confirming its regional presence in the mountains of western Gredos (Huntley, 1990; van der Knaap et al., 2005; Abel-Schaad et al., 2014). This finding represents the first record of beech from the Late Glacial in the ICS. Hornbeam (*Carpinus betulus*) has been regularly documented in Iberian pollen records during the middle and late Pleistocene (Postigo-Mijarra et al., 2008, 2010; Magri et al., 2017). Nevertheless, its presence in the Navamuño sequence ~15.6−14.5 ka cal BP is the oldest record ever recorded in the ICS, where it had only been cited from the early Holocene onwards (Atienza, 1995; Atienza et al., 1996; Abel-Schaad et al., 2014). Our data allow us to suggest the existence of Late Glacial refugia for both beech and hornbeam in the western Gredos range.

Low pollen percentages for wetland indicators, particularly of hydro-hygrophytic taxa (Figs. 5−6), are also indicative of cold and dry conditions. Between 15.6 and 14.5 ka cal BP the lithotype consists of greenish or greyish clay and clayey silt (Fig. 2; Table 1) with minimal sedimentation rate (0.23 mm yr^{-1}; Fig. 2), characteristic of a glaciolacustrine depositional environment of an amictic lake (Turu et al., 2018). This is in accordance with low MS SI units and the geochemical data (Fig. 6), which show that the main sedimentary contribution was produced by suspension, as indicated by high Al/Ti ratio (Höobig et al., 2012). Thus, relative high lake levels during the Oldest Dryas coincide with a high influence of lithogenic elements like aluminium and iron due to enhanced soil erosion related to deglaciation and with low Mn/Fe ratio (Martín-Puertas et al., 2011). Cold conditions during this period can also be inferred from the very low content (Fig. 6) of organic matter (LOI), indicative of lower organic productivity in the palaeolake (González-Sampériz et al., 2006). Similar conditions have been documented in glacial lakes of the Pyrenees, the Cantabrian

Mountains and in the Serra da Estrela at the westernmost end of the ICS during the Oldest Dryas (van der Knaap and van Leeuwen, 1997; González-Sampériz et al., 2006; Jalut et al., 2010; Oliva-Urcía et al., 2018). The presence of *Closterium idiosporum* (HdV-60) at this time would be indicative of oligo-mesotrophic open cold water conditions (van Geel, 1978; Carrión and Navarro, 2002), probably related to marked detrital inputs or to the contribution of dung from wild animals to the sedimentary basin (Carrión and Navarro, 2002; Cugny et al., 2010). In fact, low values of coprophilous fungi are also documented in LPAZ-1 (Fig. 5).

The chronology of LPAZ-1, with the exception of the upper part ~14.7−14.5 ka cal BP, is synchronous with the onset of the Oldest Dryas (Greenland Stadial 2a/GS-2a) in the Iberian mountains between 16.6 and 14.7 ka cal BP (Jalut et al., 2010; Domínguez-Villar et al., 2013; Palacios et al., 2016), a cold and dry interval documented in the Northern Hemisphere caused by the collapse of the North Atlantic Deep Water formation (Denton et al., 2006). This period has been also recorded in Greenland ice cores (Fig. 6) by very low δ^{18}O values (Rasmussen et al., 2008). The Oldest Dryas vegetation in the whole of Europe was dominated by herbs with abundant *Artemisia* and Poaceae as well as scrublands with *Juniperus* and open woodlands with *Pinus* and *Betula* trees (Watts et al., 1996; Giesecke et al., 2017; Sadori, 2018). This plant landscape is also documented in this period in pollen records of northern and southern mountains of the Iberian Peninsula, indicating cold and dry conditions with *Artemisia* and *Pinus*-*Juniperus* woods as dominant at a regional scale, but with deciduous trees in all locations (Carrión, 2002; González-Sampériz et al., 2010 and references therein; López-Merino et al., 2012; Iriarte-Chiapusso et al., 2016). At the Serra da Estrela (western ICS, Portugal), the Charco da Candieira record (1400 m asl) also shows a sedimentary sequence of soft inorganic silt ~14.8−14.7 ka cal BP, as well as a landscape dominated by herbaceous formations (*Artemisia*, Poaceae, *Plantago radicata*, Chenopodiaceae) and scarce trees (mainly *Pinus* and *Betula*), completely similar to the one described in this period in Navamuño (van der Knaap and van Leeuwen, 1995, 1997).

At Navamuño, palaeoclimate reconstruction (Fig. 6) suggests that during the Oldest Dryas the mean annual temperature (Tann) was lower that today (1.5-3 °C less). Further, the inferred total annual precipitation (Pann) indicates that climatic conditions were similar to the present ones. The few existing climate reconstructions concerning the Oldest Dryas for the whole of the Iberian Peninsula (Tarroso et al., 2016) indicate slightly cooler and drier conditions than in our reconstruction. Such cold and dry
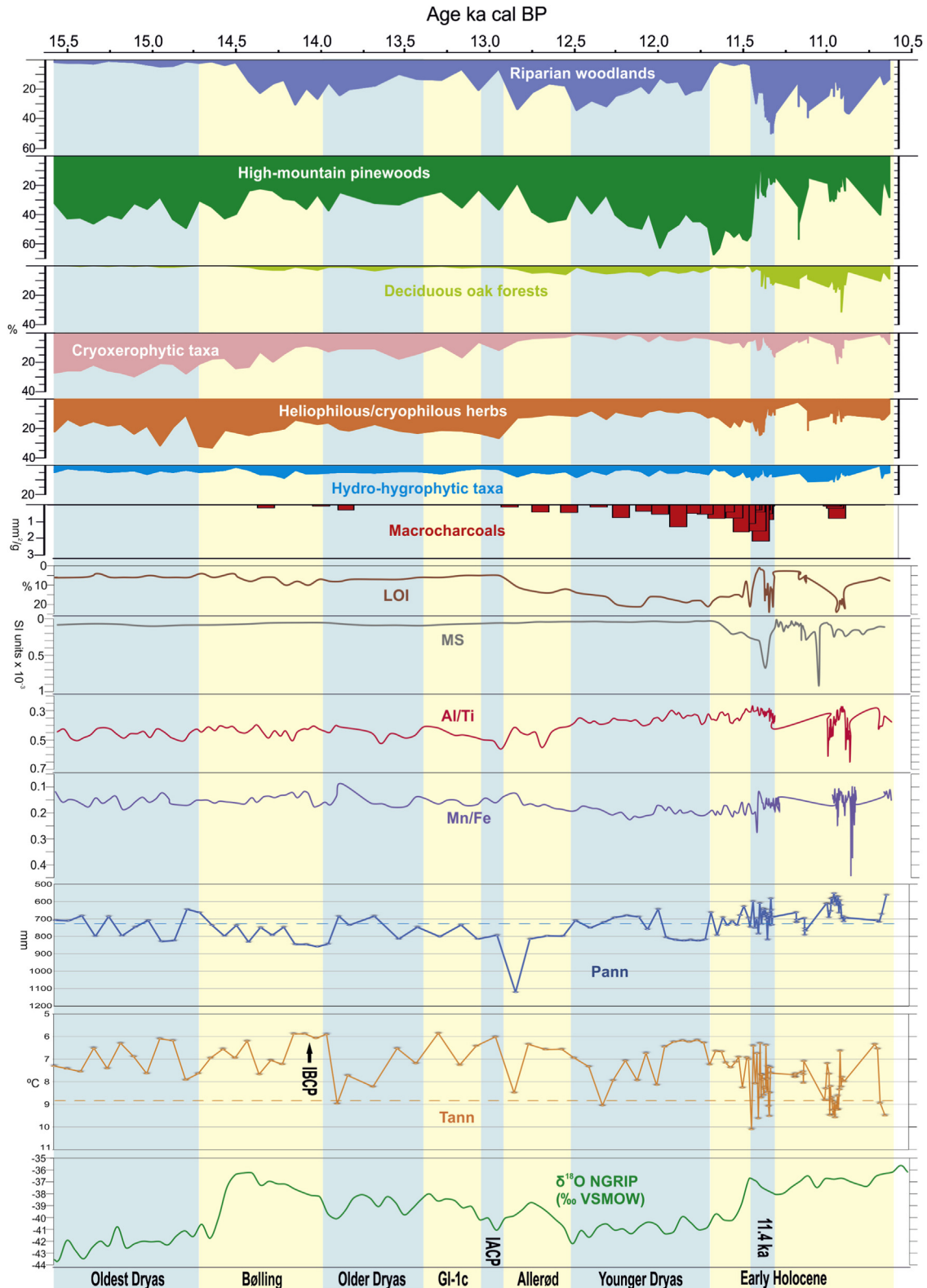
Fig. 6. Selected pollen ecological groups, macrocharcoals, organic matter content (LOI), magnetic susceptibility (MS), selected geochemical ratios, reconstructed Pann (total annual precipitation) and Tann (mean annual temperature) values of Navamuño sequence, and δ^{18}O record from NGRIP record (Rasmussen et al., 2008) plotted against age (ka cal BP). Current average climatic values (Pann and Tann) via WordlClim (dotted line) are taken as reference data for the estimated values. Color shading corresponds to climatic events mentioned in the text (IBCP: Intra-Bølling cold period; IACP: Intra-Allerød cold period). Ecological groups (see also Figs. 4–5) according to Sardinero (2004) and Abel-Shaad et al. (2014): Riparian woodlands (*Alnus, Betula, Carpinus betulus, Corylus, Frangula, Fraxinus, Salix, Tilia* and *Ulmus*); High-mountain pinewoods (*Pinus sylvestris/nigra*); Dediduous oak forests (*Quercus pyrenaica*-type); Cryoxerophytic taxa (*Artemisia*, Chenopodiaceae, *Ephedra distachya*). (For interpretation of the references to color in this figure legend, the reader is referred to the Web version of this article.)

conditions during the Oldest Dryas probably favored *Pinus nigra* over *P. sylvestris* (García-Amorena et al., 2011; Desprat et al., 2015), although in these western territories of the ICS - where oceanic influence mitigated the dryness conditions - it is likely that both pines formed mixed woodlands as it does today in the central and eastern massifs of the Gredos range in the upper supra-mediterranean bioclimatic belt (Rubiales et al., 2007; López-Sáez et al., 2016).

5.2. Bølling/Allerød interstadial (~14.7–12.6 ka cal BP)

5.2.1. Bølling sub-interstadial (~14.7–14.0 ka cal BP)

The upper part of LPAZ-1 (~14.7–14.5 ka cal BP) and LPAZ-2a (~14.5–14.0 ka cal BP) are characterized by significant changes in pollen percentages of several trees, herbaceous taxa and NPPs. According to the age-depth model (Fig. 2) the upper part of LPAZ-1 and LPAZ-2a could correlate with the Bølling sub-interstadial (Greenland Interstadial 1e/GI-1e) ~14.7–14.0 ka cal BP, which has been documented in the NGRIP Greenland core (Fig. 6) by an abrupt increase in δ^{18}O values (Rasmussen et al., 2008). *Betula* distinctly increases in LPAZ-2, while *Pinus sylvestris/nigra* and cryoxerophytic herbs gradually decrease (Figs. 3–4) and suggest the development of mixed coniferous-deciduous woodlands with *Betula* dominating the canopy. Nevertheless, *Pinus sylvestris/nigra* increases its values towards the end of LPAZ-2a ~14.1 ka cal BP. An optimum of birch woodlands has been also documented in the Pyrenees and the Alps during the Bølling oscillation (González-Sampériz et al., 2006; Giesecke et al., 2017). Trace amounts or low percentages of ever-green and deciduous *Quercus*, *Carpinus betulus*, *Corylus*, *Castanea*, *Fagus*, *Fraxinus*, *Ilex*, *Juglans*, *Tilia*, *Ulmus* and *Olea* suggest the presence of isolated stands of these trees or at least a regional presence (Huntley, 1990; van der Knaap et al., 2005; López-Sáez et al., 2010a, 2015; Broothaerts et al., 2018). A first spread of *Quercus pyrenaica*-type takes place ~14.5–14.0 ka cal BP (LPAZ-2a), starting from the Bølling sub-interstadial until the end of the Younger Dryas ~11.7 ka cal BP (Fig. 3). These facts coincide with the first step of the spread of deciduous *Quercus* throughout Europe in the Late Glacial interstadial (Brewer et al., 2002). Nevertheless, pollen records from central and southern Italian mountains, such as that from Lago Grande di Monticchio (Watts et al., 1996), Lago Trifoglietti (Beaulieu et al., 2017) and Lago di Mezzano (Sadori, 2018), already show the dominance of deciduous *Quercus* since 14.6 ka cal BP. Overall, the percentage of tree pollen increases in LPAZ-2a with respect to the previous zone. This implies that local vegetation was denser than before (>14.7 ka cal. BP) but the woodland was not yet closed. This dynamics of progressive increase in tree cover is documented by comparing the antagonistic curves of *Betula* and heliophilous/cryophilous herbs through LPAZ-2a (Figs. 3–4). The increase in tree taxa can be interpreted as a warming trend and an increase in humidity during the Bølling in the area (García-Alix et al., 2014). This interpretation is consistent with other pollen records from the Iberian Peninsula that show similar increases in high-mountain forests during the Bølling period (González-Sampériz et al., 2010; Camuera et al., 2019).

Between 14.7 and 14.0 ka cal BP, hygrophytic taxa (Cyperaceae, *Myriophyllum alterniflorum*, *Typha*) and NPPs indicators of oligo-trophic open water conditions (HdV-120, HdV-170) display higher values, which could indicate moister conditions and advances of marginal vegetation around the palaeolake (Figs. 5–6). These data agree with the abrupt decrease of cryoxerophytic herbs (Figs. 4 and 6). In particular, the increase in *Rivularia*-type (HdV-170) and Zygnemataceae (HdV-313, HdV-314, HdV-315) values would be indicative of oligo-mesotrophic conditions in the sedimentary environment (van Geel et al., 1983; López-Sáez et al., 1998; Carrión, 2002). LPAZ-2a (1557-1542 cm) is composed of dark-greenish/

greyish-brown clayey silt (Fig. 2; Table 1) probably associated to hydrophorphic soils (Turu et al., 2018) and, thus, the Navamuño palaeolake level status remained more or less stable. Constant values of the Al/Ti ratio and low MS SI units (Fig. 6) confirm that the main sedimentary contribution was produced by suspension. Nevertheless, an increase in LOI (>10%) and decreasing Mn/Fe ratio is documented at this time (Fig. 6) suggesting an increase in organic productivity, likely related to an increase in temperature and rainfall and thus, deeper lake level conditions during the Bølling oscillation.

The reconstructed Pann values in the Navamuño record (Fig. 6) show an increasing trend between 14.7 and 14.4 ka cal BP, a decrease until 14.2 ka cal BP but with an intermediate maximum ~14.3 ka cal BP, and, finally, an increasing trend until 14.0 ka cal BP. These Pann values are higher than the current ones. A similar tendency is observed in the Pann reconstruction of the Quintanar de la Sierra pollen record in northern Iberia (Ilvonen et al., 2019), as well as in the NGRIP core (Rasmussen et al., 2008). Our results are also in agreement with those presented by García-Alix et al. (2014) and Tarroso et al. (2016), who describe the Bølling oscillation as a period of increased precipitation in southern Iberia and the whole of the Iberian Peninsula, respectively. During the Bølling sub-interstadial *Fagus sylvatica* is recorded in a continuous way with somewhat higher percentages (Fig. 3). Probably, the reconstructed Pann values of greater humidity (Fig. 6) allowed the survival of beech in extra-local Late Glacial refugia of the Béjar range, partic-ularly during the Bølling oscillation as also documented in other mountains in northern Iberia (López-Merino et al., 2008; Ruiz-Alonso et al., 2019). During the Bølling, the Tann reconstruction follows a dissimilar pattern with values always lower than the current ones (Fig. 6), with an initial decrease between 14.7 and 14.4 ka cal BP, a subsequent increase until it reaches a maximum ~14.35 ka cal BP, and, finally, a decreasing trend ~14.2–14.0 ka cal BP. This last cooling phase could be tentatively correlated with the Intra-Bølling cold period-IBCP (Yu and Eicher, 2001) and the above-mentioned increase in pine forests (Fig. 6). In the ICS, the only known evidence of the Bølling sub-interstadial comes from the Charco da Candieira pollen record (1400 m asl) in the Serra da Estrela (van der Knaap and van Leeuwen, 1997). The authors of this study suggest a cool and dry climate during the first half of the Bølling sub-interstadial ~14.8–14.27 ka cal BP, and a moister and warmer one ~14.27–14.1 ka cal BP at the end, although the vege-tation dynamics is similar to that of the Navamuño record. The rainfall dynamics of the Portuguese record is also similar, while differences in temperature reconstruction may be related to the location of each core, which represent different pollen depositional and biogeographical environments (Peyron et al., 2005).

Macrocharcoal particles are only present for the upper part of the Bølling sub-interstadial (~14.3 ka cal BP), where macrocharcoal area reaches 0.2 mm^2/g (Fig. 6). These results indicate an overall low fire activity, thus, the prevalence of sufficient biomass to sus-tain fire. This is in agreement with the abovementioned greater tree cover during this oscillation, characterized by a more extensive deciduous forest spread (mainly *Betula* and *Quercus pyrenaica*). In fact, the great variability of the temperature during the Bølling oscillation did not apparently promote large wildfire ignition in Navamuño, with a single macrocharcoal peak recorded (Fig. 6). As has been explained for Pyrenean records (Gil-Romera et al., 2014), it is feasible to think that this low frequency of fires during the Bølling may be related to cool summers and very low winter temperatures.

5.2.2. Older Dryas sub-interstadial (~14.0–13.4 ka cal BP)

An important change in the vegetation composition occurred at approximately 14.0 ka cal BP (LPAZ-2b; Figs. 3–6), namely a rapid decline of *Betula*, *Salix*, *Quercus ilex* and *Juniperus* and a slight rise in

Pinus sylvestris/nigra, *Cytisus/Genista*, cryoxerophytic taxa and heliophilous/cryophilous herbs. This likely indicates a replacement of birch woodlands by high-mountain pinewoods, broom communities and grasslands until ~13.4 ka cal BP. According to the age-depth model (Fig. 2), LPAZ-2b could be correlated with the Older Dryas oscillation (Greenland Interstadial 1d/GI-1d) ~14.0−13.4 ka cal BP, which has been documented in the NGRIP Greenland core (Fig. 6) by an abrupt decrease in δ¹⁸O values (Lowe et al., 2008; Rasmussen et al., 2008). Around the palaeolake, vegetation had a low tree cover and was dominated by a steppe-like landscape, with the small transitional peak in *Alnus*, *Castanea* and *Juglans* coming from an increasing proportion of regional vegetation input from lower altitudes. As suggested by López-Sáez et al. (2013) and Broothaerts et al. (2018), it can be assumed that the frequencies of *Pinus sylvestris/nigra* observed during the Older Dryas might reflect local input from highland open pine woodlands.

The dominance of cryophilous and xerophilous herbs and the disappearance of *Fagus*, *Fraxinus* and *Ilex*, as well as the decline of most hydro-hygrophytic taxa and NPPs indicators of meso-euthropic wet/open water conditions (Figs. 3, 5 and 6) suggest cold and dry climate conditions during the Older Dryas period (Huntley, 1990). A similar picture has been documented in northern and southern Iberian territories, mainly in mountain environments (González-Sampériz et al., 2006, 2010; Morellón et al., 2009; Jalut et al., 2010; Rubiales et al., 2010; Aranbarri et al., 2014; Moreno et al., 2014; Camuera et al., 2018; Oliva-Urcía et al., 2018) including the westernmost ICS (van der Knaap and van Leeuwen, 1997). In contrast, in the mountains of the central Mediterranean (central and southern Italy), this period is characterized by an increase in tree cover (mainly of *Abies* and deciduous *Quercus* but also of other mesophilous elements) and the permanence of cryophilous and xerophilous herbs (Watts et al., 1996; Beaulieu et al., 2017; Sadori, 2018). In this period, a strong decrease of LOI is also documented at Navamuño, suggesting a substantial decrease in organic matter productivity in the palaeolake (Fig. 6).

During the Older Dryas episode the sedimentation rate increased (0.33−0.52 mm yr⁻¹; Fig. 2), probably related to increased erosion on the nearby slopes caused by a higher frequency of fires, as evidenced by a small peak (0.3 mm²/g) of macrocharcoals ~13.8 ka cal BP (Fig. 6). Although the Al/Ti ratio decreases at the beginning of this period (Fig. 6), in its upper part it reaches a maximum that would reflect, again, sedimentation fundamentally by suspension. Therefore, low fire activity around the Navamuño depression during this wooded steppe phase of the Older Dryas is consistent with the interpretation of low fuel availability on the Iberian Peninsula during stadial o cold sub-interstadial periods (Daniau et al., 2007).

At this time (1542-1520 cm), sedimentation in the Navamuño depression changed from lacustrine dark-grey-brown clayey silt during the Bølling sub-interstadial to dark green silty clay with the onset of the Older Dryas (Fig. 2; Table 1). These sediments present the typical coloring of reductive sedimentary conditions (Turu et al., 2018). This discoloration occurs when the redox potential is low and there is leaching by the phreatic surface of chromogenic compounds such as Fe and Mn, suggesting deeper and poorly oxygenated mixed water conditions in the palaeolake (Haliuc et al., 2017). Fluctuations in Fe and Mn content in the sediments have been commonly interpreted as a reflection of mineral input variability (clays, heavy metals and oxides), and as changes in redox conditions in lake environments because of their different responses to oxygen conditions (Naeher et al., 2013). Thus, increasing water inflow in the Navamuño palaeolake during the onset of the Older Dryas is supported by very low Mn/Fe values (Fig. 6), which would suggest accordingly deeper and poorly oxygenated mixed water conditions (Davison, 1993). Subsequently, the Mn/Fe ratio

increases again until ~13.3 ka cal BP (Fig. 6) pointing to lower better oxygenated waters. These facts agree with a maximum of HdV-120 indicating a lake deposit, but not in an optimal lake's earliest phase (Pals et al., 1980).

The Older Dryas (~14.0−13.4 ka cal BP) was a drier period than the previous Bølling oscillation but similar to the current conditions. Pann values show a decreasing trend until ~13.7 ka cal BP and then a growing pattern until ~13.4 ka cal BP (Fig. 6). Mean annual temperatures also show a marked difference increasing to a maximum value ~13.9 ka cal BP, and then declining abruptly until ~13.4 ka cal BP (Fig. 6). Nevertheless, it is interesting to note that although Tann values show a clearly decreasing pattern during the Older Dryas, its values are generally higher than those of the Bølling oscillation but significantly lower than the current ones. These facts can be interpreted within the general trend of global warming associated with the Bølling/Allerød interstadial in southern Europe (Morellón et al., 2009; Carrión et al., 2010; González-Sampériz et al., 2010; Rodrigo-Gámiz et al., 2011; Moreno et al., 2014; Beaulieu et al., 2017; Sadori, 2018).

5.2.3. Allerød sub-interstadial (~13.4−12.6 ka cal BP)

5.2.3.1. Greenland interstadial 1c (~13.4−13.1 ka cal BP) and Intra-Allerød cold period (~13.1−12.9 ka cal BP).
In the first half of the LPAZ-2c sub-zone (1520-1515 cm; 13.4−13.1 ka cal BP), *Pinus sylvestris/nigra*, *Betula* and *Salix* pollen percentages rapidly increase, although those of birch and willow are then significantly reduced, whereas those of *Alnus*, evergreen and deciduous *Quercus* increase (Fig. 3). In contrast, in the second half of LPAZ-2c (1515-1500 cm; 13.1−12.9 ka cal BP), *Betula* pollen percentages progressively increase, whereas those of *Pinus sylvestris/nigra* and *Quercus ilex* decline, suggesting that *Pinus*-dominated woodlands were replaced by mixed pine-birch woodlands and that regionally meso-mediterranean oak forests were reduced probably in favor of degrading serial stages consisting of rockrose (*Cistus*-type) (Figs. 3−6). The walnut tree (*Juglans regia*) is continuously present throughout the LPAZ-2c sub-zone, while *Corylus*, *Tilia* and *Ulmus* are only present from ~13.1 ka cal BP (Fig. 3), suggesting the existence of refuge areas for these species in the southern valleys of the Béjar range (López-Sáez, 1993; López-Sáez and López-García, 1994; Abel-Schaad et al., 2014). Heliophilous/cryophilous herbs are also more abundant from ~13.1 ka cal BP.

In the second half of LPAZ-2c sub-zone, pollen of aquatic plants and wetland taxa slightly decrease (Figs. 5−6), suggesting they were dominant around the lake shore only ~13.4−13.1 ka cal BP. Similarly, within the NPPs (Figs. 5−6), the first half of the sub-zone is characterized by the dominance of *Rivularia*-type (HdV-170), while the second is dominated by HdV-120, HdV-174 and Zygnemataceae (HdV-313, HdV-314, HdV-315), suggesting a change in the lake trophic conditions from oligotrophic open water conditions ~13.4−13.1 ka cal BP to meso-eutrophic ones at the end ~13.1−12.9 ka cal BP (Pals et al., 1980; van Geel et al., 1983; López-Sáez et al., 1998).

According to the age-depth model (Fig. 2) the lower part of LPAZ-2c could correlate with the Greenland Interstadial 1c (GI-1c) ~13.4−13.1 ka cal BP, while the upper part of the sub-zone could be tentatively correlated with the Intra-Allerød cold period (IACP; Greenland Interstadial 1b/GI-1b) ~13.1−12.9 ka cal BP (Yu and Eicher, 2001; González-Sampériz et al., 2006), which have been documented in the NGRIP Greenland core (Fig. 6) by an abrupt increase and a subsequent decrease in δ¹⁸O values, respectively (Rasmussen et al., 2008). LPAZ-2c is composed of dark green silty clay (Fig. 2; Table 1), probably associated to hydromorphic soils (Turu et al., 2018).

During the GI-1c sub-interstadial and the IACP (Fig. 6), the inferred Pann values are slightly higher than the current ones

(about 100 mm). These Pann values are very similar to those documented during the Bølling oscillation. Nevertheless, the reconstructed Tann values during the GI-1c sub-interstadial abruptly increase from a minimum ~13.3 ka cal BP to a maximum ~13.1 ka cal BP. Then they decrease sharply during the IACP (Fig. 6), suggesting the shift from more thermal climatic conditions to colder ones around 13.1 ka cal BP. These climatic trends could explain the development of high-mountain pine forests, acting as pioneers during the GI-1c warm period. A temperature increase is also marked during the GI-1c sub-interstadial by increasing percentages of hydro-hygrophytic herbs and a greater abundance of coprophilous fungi (Figs. 5–6) that could probably be related to a greater influence of wild fauna in the environment of the palae-olake installed in the Navamuño depression (Carrión, 2002; Carrión and Navarro, 2002; López-Sáez and López Merino, 2007). On the other hand, a progressive trend towards colder conditions during the IACP would have meant the development of birch woods to the detriment of pine forests, reducing the hydro-hygrophytic herba-ceous cover around the lake and changing its trophic conditions from oligotrophic to meso-eutrophic ones. The increase in helio-philous/cryophilous herbs during the IACP is also a proof of the decrease in temperature.

During the IACP the Al/Ti ratio increases while the Mn/Fe ratio slightly decreases (Fig. 6). Thus, the IACP could be considered as a similar period to the abovementioned Older Dryas but of lesser magnitude in the palaeoclimatic evolution of the study area. Therefore, we can interpret the Mn/Fe ratio as a proxy for the Navamuño palaeolake level oscillation where increasing values during the GI-1c sub-interstadial depict an oxygenated environ-ment under lower lake levels, while decreasing ones during the IACP suggest poorly oxygenated water and higher lake levels (Davison, 1993; Haliuc et al., 2017; Oliva-Urcía et al., 2018).

5.2.3.2. Allerød oscillation (~12.9–12.6 ka cal BP).
A notable in-crease in tree pollen percentages is documented in the lower part of the LPAZ-3a (1500-1485 cm) pollen sub-zone ~12.9–12.6 ka cal BP (Fig. 3). In this period, high-mountain pines, broom communities and junipers as well as some deciduous trees and Pinus pinaster develop, while Betula abruptly decreases. Cryoxerophytic and heliophilous/cryophilous taxa also reduce their percentages at this time, while hygrophytic taxa increase significantly (Figs. 4–6). These data suggest warmer and wetter climatic conditions, which accordingly to the age-depth model (Fig. 2) could correlate with the Allerød episode (Greenland Interstadial 1a/GI-1a) ~12.9–12.6 ka cal BP, which has been documented in the NGRIP Greenland core (Fig. 6) by an increase in $\delta^{18}O$ values (Rasmussen et al., 2008). A similar pattern has been documented in Pyrenean, Cantabrian, Southern Iberian and Baetic pollen records from Iberian mountain areas during the Allerød warm period, including the development of high-mountain pine forests and junipers acting as pioneers (Carrión, 2002; González-Sampériz et al., 2006, 2010; Aranbarri et al., 2014; Rubiales et al., 2010; Iriarte-Chiapusso et al., 2016), as well as the reappearance of beech in the pollen records (López-Merino et al., 2008; Ruiz-Alonso et al., 2019).

The reconstructed Pann and Tann values during the Allerød oscillation clearly show an increase in both rainfall and tempera-ture, with maximum values ~12.8 ka cal BP, although these later decrease (Fig. 6). Anyway, Pann values are always higher (100–400 mm) than the current ones, while Tann values are always lower. This climatic improvement, that allowed rapid forest recolonization by a general development of high-mountain pine forests, has been documented in all European mountain areas (Watts et al., 1996; Ammann et al., 2007; Beaulieu et al., 2017; Giesecke et al., 2017). Therefore, it suggests a warming trend from the Bølling to the Allerød period that has also been evidenced in

both marine and terrestrial records in the southern Mediterranean region (Watts et al., 1996; Naughton et al., 2007, 2019; Lowe et al., 2008; González-Sampériz et al., 2010; Moreno et al., 2014; Beaulieu et al., 2017; Sadori, 2018). In summary, in the Navamuño depres-sion, it can be assumed that pioneer open pine woodlands were developing in the vicinity of the palaeolake during the Allerød oscillation. However, in the Serra da Estrela, the Allerød episode was characterized by increasing values of both pine and birch (van der Knaap and van Leeuwen, 1997), likely related to a greater in-fluence of wet winds from the Atlantic Ocean in these westernmost territories of the ICS (Abel-Schaad et al., 2014). It is also interesting to note the expansion of both evergreen and deciduous Quercus (Figs. 3 and 6) in response to the Allerød oscillation (Björck et al., 1997), which fully agrees with other Iberian and southern Medi-terranean areas where a broadleaved forest expansion has been recognized (Watts et al., 1996; Pons and Reille, 1988; Brewer et al., 2002; González-Sampériz et al., 2006; López-Merino et al., 2008, 2012; Iriarte-Chiapusso et al., 2016; Beaulieu et al., 2017; Camuera et al., 2018, 2019; Sadori, 2018).

During the Allerød oscillation the Al/Ti and Mn/Fe ratios follow antagonistic trends. The former shows a declining but oscillating pattern, while the latter displays a growing trend, as does LOI (Fig. 6), suggesting better oxygenated waters with a lower contri-bution of terrigenous elements, low lake levels and higher organic productivity in the palaeolake (González-Sampériz et al., 2006; Haliuc et al., 2017). Although with low values (0.12–0.44 mm²/g), macrocharcoal particles are continuously present during the Allerød oscillation ~12.9–12.6 ka cal BP (Fig. 6), probably indicating an overall low fire activity, which is in agreement with the abovementioned increase in tree cover during this warm episode. A similar trend in the frequency of fires has been documented in the Serra da Estrela during this period (Connor et al., 2012). The regionally homogeneous pattern in biomass burning in the western ICS suggests modulation from a large-scale driver, namely the climate regime. According to Gil-Romera et al. (2014), during this warm interval summer temperature progressively increased, leading to a parallel increase in fire frequency, supporting this climatically driven character of these fires. Human societies had no or little and localized influence on regional fire and vegetation dynamics during this time interval, since only one relatively remote Upper Palaeolithic archaeological site (Fig. 1) have been docu-mented in the Béjar range, which corresponds to a hunter's camp (La Dehesa) of the Upper Magdalenian (Hernández-Díaz and Avilés-Amat, 2013).

5.3. Younger Dryas stadial (~12.6–11.7 ka cal BP)

The upper part of the LPAZ-3a pollen sub-zone (1485-1420 cm) is marked by a transitional reversal of the Betula curve after a maximum reached ~12.5 ka cal BP, while frequencies of cryoxer-ophytic taxa and heliophilous/cryophilous herbs, Cytisus/Genista, Juniperus and Lamiaceae reach higher values ~12.6–11.7 ka cal BP (Figs. 3, 4 and 6). Maximum values of Betula have also been docu-mented in the Lago Trifoglietti and Lago Grande di Monticchio pollen records (southern Italy) ~12.5–12.4 ka cal BP (Watts et al., 1996; Beaulieu et al., 2017). Although following an oscillating curve, the percentages of Pinus sylvestris/nigra show an increasing trend reaching maximum values ~12.1–11.9 ka cal BP (Fig. 3). Such assemblages indicate a local extent of high-mountain pine forests with broom communities and junipers (López-Sáez et al., 2013; Giesecke et al., 2017; Broothaerts et al., 2018), as well as the development of cold steppe grasslands linked with a decline of birch woodlands in the area. Regional beech (Fagus sylvatica) populations are maintained and even appear to be increasing, like in other pollen records in the north of the Iberian Peninsula

~12.6—11.7 ka cal BP (López-Merino et al., 2008; Ruiz-Alonso et al., 2019). This reversal in the vegetation dynamics has been typically recorded during the Younger Dryas cold and dry event (Greenland Stadial 1/GS-1) in northern and southern mountain Iberian pollen records (Pons and Reille, 1988; Carrión, 2002; Muñoz-Sobrino et al., 2004, 2013; González-Sampériz et al., 2006, 2010; Carrión et al., 2010; Moreno et al., 2011; López-Merino et al., 2012; Morales-Molino and García-Antón, 2014; García-Ruiz et al., 2016; Iriarte-Chiapusso et al., 2016; Camuera et al., 2018). This is in agreement with the Navamuño age-depth model, which places the top of the LPAZ-3a pollen sub-zone ~12.6—11.7 ka cal BP (Fig. 2). Nevertheless, sequences from other Iberian Mediterranean continental and southern Italian mountain areas generally show little changes in vegetation composition and the persistence of conifers, deciduous oaks and open landscapes (Watts et al., 1996; Aranbarri et al., 2014; Beaulieu et al., 2017). The Younger Dryas is clearly recorded in Greenland ice cores (Fig. 6) by low and oscillating $\delta^{18}O$ values (Alley, 2000; Rasmussen et al., 2008), as well as in many other palaeoenvironmental studies across the western Mediterranean (Morellón et al., 2009; Fletcher et al., 2010; Moreno et al., 2014; Tomasso et al., 2018; Naughton et al., 2019).

The Younger Dryas was locally characterized by a lake-level drop, as indicated by the return towards the deposition of dark brown silty clay (Fig. 2; Table 1). The greater abundance of organic matter - with two LOI maximum values ~12.2 ka cal BP (1458 cm) and 11.45 ka cal BP (1379 cm) (Fig. 6) - gives the sediment their characteristic dark brown color, interpreted as a marshy environment (Turu et al., 2018). A sharp decrease in Al/Ti ratio and a moderate reduction in MS (Fig. 6) corroborate this hypothesis. During the early Younger Dryas, the Mn/Fe ratio increases until ~12.2 ka cal BP (Fig. 6) pointing to lower and better oxygenated waters (Haliuc et al., 2017). The surface enrichment in Mn is probably related to vadose oxic conditions ~12.6.-12.2 ka cal BP, which involve more favorable conditions for oxidized, less mobile forms of these elements to form (Chesworth et al., 2006). Lower LOI values and decreasing ones of the Mn/Fe ratio ~12.2—11.7 ka cal BP (late Younger Dryas) support the idea of greater water saturation of sediments (Fig. 6), deeper but less oxygenated water (Davison, 1993; Haliuc et al., 2017). Around the marsh, vegetation was probably forested and dominated by pines and a steppe-like landscape, with the still important presence of both deciduous and evergreen oaks (Quercus pyrenaica and Quercus ilex pollen types), beech (Fagus sylvatica) and hazel (Corylus) resulting in an increasing proportion of regional vegetation input from lower altitudes (López-Sáez et al., 2010a, 2015; Abel-Schaad et al., 2014). In addition, the increase in Pinus sylvestris/nigra at this time may partially reflect an altitudinal migration of the pinewood treeline associated with the onset of cooler conditions at high elevations (Aranbarri et al., 2014). During the Younger Dryas some hydro-hygrophytic herbs develop thanks to the installation of the aforementioned marsh-type environment (Figs. 5—6). Meanwhile, the phreatic level decrease, which could even have meant the possible desiccation and sub-aerial exposure of the site, would have led to the disappearance of all NPPs (Fig. 5).

The transition to the Younger Dryas is characterized by a rapid decrease in Pann values ~12.6—12.0 ka cal BP followed by an abrupt increase until 11.7 ka cal BP (Fig. 6). The Tann curve from Navamuño core shows that the first part of the Younger Dryas ~12.6—12.0 ka cal BP was warmer than the second one ~12.0—11.7 ka cal BP (Fig. 6). The palaeoclimatic reconstruction then suggests dry and warm conditions for the first part of the Younger Dryas and wetter and cooler ones for the second one. This pattern is in agreement with the results obtained by Ilvonen et al. (2019), who document drier conditions during this period than in the previous Allerød sub-interstadial. van der Knaap and van Leeuwen (1997) cite a dry

and cool climate in the first part of the Younger Dryas ~12.85—11.87 ka cal BP at Serra de Estrela, followed by a moister and warmer period at the end of the Younger Dryas ~11.87—11.63 ka cal BP. Aranbarri et al. (2014) and Wei et al. (2019), as in the Navamuño sequence, point to wetter conditions for the second part of the Younger Dryas ~12.2—11.7 ka cal BP in the Villarquemado palaeolake record (Southern Iberian Range). Similar to our data, Morellón et al. (2018) also document two climatic phases within the Younger Dryas in their synthesis of the Iberian Peninsula, emphasizing the great existing spatial variability of palaeoclimatic and palaeohydrological conditions during the GS-1, besides the generalized occurrence of cold and arid conditions. These conditions have been recorded in northern Iberian lacustrine records during the Younger Dryas (Moreno et al., 2011; Muñoz-Sobrino et al., 2013; Iriarte-Chiapusso et al., 2016). By contrast, the Sanabria lake (northwestern Iberia) shows a more complex pattern (Muñoz-Sobrino et al., 2004), including a first colder and wetter phase ~12.9—12.4 ka cal BP followed by a subsequent warmer and driest one ~12.4—11.7 ka cal BP. A biphasic structure of the Younger Dryas has been also recorded in the speleothem sequence of Seso Cave (Southern Pyrenees), with an initial phase ~12.9—12.5 ka cal BP characterized by dry conditions, followed by a progressive increase in humidity and warmer conditions until 11.7 ka cal BP (Bartolomé et al., 2015). A similar variability was found in La Garma Cave (Cantabrian Mountains), with a more direct influence of the westerlies ~12.85—12.15 ka cal BP, and milder conditions afterwards (Baldini et al., 2015). In general, Mediterranean littoral areas recorded markedly arid conditions during most of the Younger Dryas, either in two phases or in a more continuous pattern, especially remarkable in its second half (Morellón et al., 2018). In short, the palaeoclimatic reconstruction of Navamuño offers yet another proof of the great variability that exists within the Younger Dryas. Despite its location in the Mediterranean region, this record shows the same variability as others documented in the north and northwest of the Iberian Peninsula within the Eurosiberian biogeographical region. Probably, the location of the Navamuño sequence at the westernmost end of the ICS, as well as the influence exerted by the proximity of the Atlantic Ocean, could explain these facts.

Enhanced and continued fire activity along with an increasing sedimentation rate ($0.85–1.18$ mm yr^{-1}) is evident during the Younger Dryas stadial ~12.6—11.7 ka cal BP (Figs. 2 and 6), with maximum macrocharcoal values (1.3 mm^2/g) and a maximum peak of Asphodelus albus ~11.9 ka cal BP (Fig. 4), coinciding with the abovementioned more extensive high-mountain pine forest spread. At the westernmost end of the ICS, a similar period of increased but low fire activity has been documented in the Serra da Estrela ~12—11 ka cal BP, which has been interpreted as a phase of low fuel availability related to steppe-type vegetation (Connor et al., 2012). One explanation for the observed pattern at Navamuño record is that a dry and warm climate during the first half of the Younger Dryas ~12.6—12.0 ka cal BP may have increased the tree and shrub mortality (with minimum values of Pinus sylvestris/nigra and a progressive decrease of the Betula curve; Fig. 3), whereas an important temperature decline (~2 °C) and high moisture availability ~12.0—11.7 ka cal BP likely promoted ignition and fire spread. An increase in fire activity at the end of the Younger Dryas has been also documented for Central Europe and North America linked to high tree mortality (Marlon et al., 2009; Feurdean et al., 2012). Nonetheless, the composition of vegetation and flammability of forest species may have also acted as a significant driver of fire activity in the western Gredos range (Viedma, 2008; Moreno-Rodríguez et al., 2011). For example, pollen and macrocharcoal records from the ICS suggest that increasing fire activity coincides with periods with greater biomass availability,

namely with the expansion of *Pinus sylvestris/nigra* forests under wetter climate conditions (Morales-Molino et al., 2013; López-Sáez et al., 2018a, 2018b). Although vegetation burning is more frequently documented in warm and dry periods, fire events are often preceded by wetter conditions that favor biomass up-take (Daniau et al., 2007; Zumbrunnen et al., 2009; Camarero et al., 2018; Sangüesa-Barreda et al., 2019).

5.4. Early Holocene (~11.7−10.6 ka cal BP)

5.4.1. The expansion of pine forests during the early Preboreal (~11.7−11.45 ka cal BP)

Distinct vegetation changes occurred around ~11.7−11.45 ka BP (LPAZ-3b), when *Pinus sylvestris/nigra*, *Cytisus/Genista* and *Juniperus* quickly expanded on the slopes surrounding the site, accompanied by a sudden decrease of *Betula*, *Corylus*, *Fagus sylvatica* and *Quercus* species (Fig. 3). These data suggest the development of high-mountain pine forests enriched in broom communities and crawling junipers (Rubiales et al., 2007, 2010; López-Sáez et al., 2013; García-Álvarez et al., 2017; Broothaerts et al., 2018). According to the age-depth model (Fig. 2), the timing of the marked changes coincides with the late Pleistocene/Holocene transition ~11.7 ka cal BP (early Preboreal), which is expressed as a rapid temperature rise in many European pollen records (Björck et al., 1997; Giesecke et al., 2017), as well as by an abrupt increase in $\delta^{18}O$ values (Fig. 6) in the NGRIP Greenland core (Rasmussen et al., 2008). The vegetation around Navamuño seems to have responded almost instantaneously to this climate change by a rapid high-mountain reforestation and a dramatic reduction of open vegetation communities (Fig. 3) and birch woodlands. However, the relative high amount of cryoxerophytic and heliophilous/cryophilous taxa suggest the presence of some tree patches dominated by steppe-like communities (Figs. 3, 4 and 6). A similar pattern has been documented in northern, southern and eastern Iberian pollen records, where the existence of high-mountain pine forests at the very beginning of the early Holocene is basically a consequence of altitude, continentality and aridity in mountain areas (Carrión, 2002; Carrión et al., 2010; González-Sampériz et al., 2010; Rubiales et al., 2010; Aranbarri et al., 2014). Palynological records from the Serra da Estrela show a broadly similar trend of vegetation reforestation for the early Holocene (van der Knaap and van Leeuwen, 1997), although woodland was composed of *Betula*, *Salix* and *Frangula*. This is not surprising considering that in the westernmost sector of the ICS the continentality is buffered by the oceanic influence coming from the west (van der Knaap and van Leeuwen, 1997; Gavilán, 2005). Similarly, some pollen records from southern Italian mountains also show the abundance of birch in the early Preboreal as well as the permanence of cryoxerophytic taxa although following a decreasing pattern (Watts et al., 1996; Beaulieu et al., 2017).

Drier conditions could be also inferred from decreasing wetland taxa, possibly as a response to higher temperatures, although the maintenance of *Alisma*, Cyperaceae, *Epilobium* and *Myriophyllum alterniflorum* (Fig. 5) probably suggests the local existence of a floodplain with stagnant shallow water (Carrión, 2002). In fact, the Navamuño record (Fig. 2; Table 1) indicates at this time (~11.7−11.45 ka cal BP; 1420-1375 cm) the transition from dark green silty clay to sands mixed with dark brown silt, as well as a constantly increasing sedimentation rate (1.18−1.47 mm yr^{-1}), suggesting a new basel-level rise after the Younger Dryas, probably indicative of the installation in the Navamuño depression of a shallow lagoon, or more likely, a floodplain, since the appearance of paleosols does not allow us to suppose the existence of a lake (Carrasco et al., 2018). Confirming these facts, in this period both Al/Ti and Mn/Fe ratios show a decreasing pattern, like LOI values,

while MS progressively increase (Fig. 6), suggesting a greater saturation in water of the sediments, particularly of coarse silts and sand size fractions, and reduced detrital input (Kylander et al., 2011). An immediate recovery of lake levels after the Younger Dryas has been also documented in most records of the Iberian North, while those of the Mediterranean region document a general decrease in lake level (Morellón et al., 2018). The Navamuño hydrological history shares aspects of both trends but resembles more closely records from northern sites.

The early Holocene ~11.7−11.45 ka cal BP is characterized at Navamuño by a rise in the Tann values compared to the previous Younger Dryas stadial (Fig. 6), clearly showing the progressive warming that occurred at the onset of the Holocene with values even higher than the current ones. On the other hand, Pann values show a relatively constant pattern (Fig. 6), although in general with values lower than those documented in the final part of the Younger Dryas and today, suggesting therefore relatively more arid conditions. These values are close to that reconstructed from pollen data at Quintanar de la Sierra in the Northern Iberian System (Ilvonen et al., 2019).

Our data indicate great fire activity at the beginning of the early Holocene ~11.7−11.45 ka cal BP (Fig. 6). The increasing trend of MS SI units is probably related to fires that occurred in the Navamuño depression, as evidenced by the substantial increase in macro-charcoals (Fig. 6), but could be also related to wetter conditions suggesting that runoff dominated over aeolian processes at this time (Mesa-Fernández et al., 2018). Interestingly, the increase in biomass burning at Navamuño from ~11.7 ka cal BP is earlier than in most other south-western European records, where it occurred mainly after 11.3 ka cal BP (Carrión, 2002, Carrión, 2012; Vannière et al., 2008, 2010, 2011; Gil-Romera et al., 2010a, 2014; Connor et al., 2012, 2019; Burjachs and Expósito, 2015). We can therefore suggest that the development of high-mountain pine forests and broom communities during the early Holocene in the western ICS and their rapid postglacial expansion imply substantial biomass availability already at the onset of the Holocene. This rise in fire activity also coincides with a large increase in the atmospheric CO_2 (Harrison and Prentice, 2003) and a massive decline in herbivores pressure (coprophilous fungi were not recorded at this time) and both could have further lead to a biomass increase. Higher *Asphodelus albus* percentages (Fig. 4) are also indicative of the above-mentioned higher frequency of fires (Abel-Schaad and López-Sáez, 2013).

5.4.2. The abrupt climate event ~11.4 ka cal BP (Preboreal oscillation)

The previous described trend is abruptly altered ~11.45−11.3 ka cal BP (bottom of LPAZ-4; 1375-1330 cm) as demonstrated by maximum values of *Betula*, *Alnus*, *Quercus ilex*, *Quercus pyrenaica*, *Juglans*, *Corylus*, *Fagus sylvatica*, Lamiaceae, *Juniperus*, *Cytisus/Genista*, *Ephedra distachya* and *Erica australis* and a clearly decreasing pattern of *Pinus sylvestris/nigra* (Fig. 3). Among herbs (Fig. 4), cryoxerophytic, heliophilous/cryophilous elements and others herbs typical of open spaces and sandy soils increase their values, suggesting the development of cryophilous and heliophilous herbaceous communities in the vicinity of the site. These data are consistent with the increase of most hydro-hygrophytic taxa and both Filicales monolete and trilete (Figs. 5−6). Fairly high pollen percentages for riparian woodland and wetland indicators (Fig. 6) indicate that these communities developed around the margins of the depression, particularly the birch, thanks to its pioneering and heliophilous character, suggesting the development of open mixed woodland dominated by *Betula* and *Pinus sylvestris/nigra* with broom communities, crawling junipers and heaths (García-Álvarez et al., 2017; Broothaerts et al., 2018). This abrupt change is also

recorded by maxima values of Al/Ti and Mn/Fe ratios, higher values of macrocharcoals, a maximum of MS ~11.37 ka cal BP (1350 cm) and a marked peak of LOI values ~11.35 ka cal BP (1340 cm) (Fig. 6). All these facts are coherent with a new base-level drop and dominant ephemeral lake conditions, producing an increase of lithogenic elements by detrital input, especially of sands from the neighboring sedimentation basin (Fig. 2; Table 1), as a result of erosive processes associated both with the decrease in base-level and the recurrence of local fires (Koinig et al., 2003; Haliuc et al., 2017). Maximum *Glomus* values (Fig. 5) can be also interpreted as a result of the abovementioned erosive events (Carrión and Navarro, 2002). The sharp rise in percentage of *Typha angustifolia* and the presence of NPPs indicators of meso-eutrophic wet/open water conditions (Fig. 5) could indicate a shallow basin environment (López-Sáez et al., 1998; Carrión and Navarro, 2002).

According to the age-depth model (Fig. 2), the aforementioned data can be correlated with the so-called 11.4 ka cal BP abrupt climatic event characterized by dry continental and cool conditions (van der Plicht et al., 2004). This phase was coeval with the coldest part of the Preboreal oscillation (Fig. 6) as observed in the $\delta^{18}O$ record of the Greenland ice-core record (Björck et al., 1997; Rasmussen et al., 2008), attributed to a large meltwater flux that resulted in a temporary decrease of the thermohaline circulation in the North Atlantic (Fisher et al., 2002). This climate reversal has been already documented in northern and eastern Iberian pollen records (González-Sampériz et al., 2010; Burjachs et al., 2016; Iriarte-Chiapusso et al., 2016) although this is the first evidence in the Spanish Central System. In the Serra da Estrela, van der Knaap and van Leeuwen (1997) document this oscillation ~11.49–11.05 ka cal BP by a halt in tree expansión and low lake levels.

The paleotemperature record at Navamuño (Fig. 6) shows a first slight cooling at around 11.45–11.43 ka cal BP, then a strong increase ~11.42 ka cal BP, and finally a progressive decrease until 11.3 ka cal BP. The 11.4 ka cal BP event in the Navamuño record is characterized by a marked peak in the Pann values ~11.45 ka cal BP, followed by a progressive decline until 11.41 ka cal BP, and finally a new marked peak ~11.33 ka cal BP (Fig. 6). Pann values are generally lower than those documented during the second half of the Younger Dryas. Greater aridity conditions are also illustrated by maxima of NPPs indicators of local dry conditions (Fig. 5), particularly *Pleospora* sp. (HdV-3B), *Triglocladium opacum* (HdV-10) and HdV-20 (van Geel, 1978). The aforementioned decrease in lake level would probably favor wildlife access to the Navamuño depression, hence the increase in coprophilus fungi values (Fig. 5).

Increasing fire activity is documented during the 11.4 ka cal BP event (maximum macrocharcoal values: 2.18 mm²/g), coinciding with the development of birch woodlands and *Asphodelus albus* (Figs. 5–6). A similar period of increasing fire frequency has been documented in the Serra da Estrela ~11.4–11.3 ka cal BP (Connor et al., 2012). Although some authors consider that human communities of the Mesolithic could have favored early Holocene fires (Ryan and Blackford, 2010), no archaeological site of this chronology has so far been documented in the study area (Hernández-Díaz and Avilés-Amat, 2013). The long-term role of birch in the supramediterranean bioclimatic belt of the Gredos range is in agreement with its documented early-successional character after disturbances, as revealed by other Holocene sequences (Atienza et al., 1996; Abel-Schaad et al., 2014; López-Sáez et al., 2014; García-Álvarez et al., 2017) and ecology studies on its resprouting ability (Reyes and Casal, 1998). Interestingly, *Betula* in Navamuño was a main factor in building up fuel during the 11.4 event but its development was negatively affected by fire at the beginning of the early Holocene and immediately after the abovementioned abrupt event (Fig. 6). This fact is common with most mountain trees, supporting the idea of the high-mountain ecosystem as a long-term

fire-sensitive environment (Gil-Romera et al., 2014).

5.4.3. Climate instability during the late Preboreal (~11.3–10.6 ka cal BP)

The late phase of the early Holocene ~11.3–10.6 ka cal BP in the study area was still characterized by open mixed woodlands dominated by *Betula* and *Pinus sylvestris/nigra* with broom communities, crawling junipers and heaths (top of LPAZ-4; 1330-707 cm). However, during this period the antagonistic pattern followed by birch and pine, with three maxima for the former (~11.17, 11.11, and 10.87 ka cal BP) and another three for the latter (~11.16, 10.98, and 10.7 ka cal BP), is very noticeable (Fig. 3). Usually, maximum birch values are concomitant with maximum *Alnus glutinosa* and *Tilia* percentages (Fig. 3). This increase of more water-demanding temperate taxa such as birch, alder and lime suggests increasing temperature and humidity (Aranbarri et al., 2014), while maximum values for pine would be indicative of greater continentality and drier conditions (López-Sáez et al., 2013; Broothaerts et al., 2018). Therefore, the greatest difference between the top and the bottom of LPAZ-4 is a sudden shift to a more humid climate when riparian woodlands expanded again ~11.3 ka cal BP at the beginning of the late Preboreal. This is consistent with the percentage increase of most hydro-hygrophytic taxa and NPPs indicators of oligo-mesotrophic open water conditions such as *Rivularia*-type (HdV-170), which presents maximum values ~10.9–10.8 ka cal BP (Fig. 5).

Between 11.3 and 10.6 ka cal BP, a clear vegetation change occurred also in the Navamuño depression lowlands, with the spread of broadleaved vegetation, both deciduous and evergreen *Quercus* (Figs. 3 and 6). A similar picture has been documented in the Serra da Estrela ~11.05–10.52 ka cal BP (van der Knaap and van Leeuwen, 1997), suggesting denser woodlands and the first arrival of oaks near the Navamuño depression as a result of climatic warming (Brewer et al., 2002; Carrión et al., 2010; López-Sáez et al., 2015). In fact, maximum values for *Quercus pyrenaica* ~11.68 and 10.91 ka cal BP coincide with minimum percentages of birch throughout this period (Fig. 3), probably indicating that deciduous oaks became dominant and birches were restricted to moist habitats (García-Álvarez et al., 2017). Thus, the beginning of the Holocene forest recovery was very pronounced as in many other Iberian and southern Mediterranean pollen records, where tree populations expanded dramatically in response to warmer and wetter climate (Watts et al., 1996; Carrión et al., 2010; Carrión, 2012; Beaulieu et al., 2017; Sadori, 2018). The oscillating dynamics of the *Quercus pyrenaica* curve suggests that deciduous oak expansion may have occurred in pulses, rather than as a gradual rise (van der Knaap and van Leeuwen, 1997).

The anomalous increase in sedimentation rate from 1330 to 785 cm (~11.3–10.95 ka cal BP), which reaches average values of 14.89 mm yr⁻¹ and maximum of 100 mm yr⁻¹–11.12 ka cal BP (Fig. 2), clearly marks a sudden change in the sedimentary regime (Turu et al., 2018). Probably, this anomalous sedimentation could be correlated with the environmental and geomorphological destabilization of the Navamuño depression after the abovementioned 11.4 ka cal BP abrupt event. This segment of the sequence is initially characterized by coarse sand, which subsequently transitions to dark brown silts ~11.05 ka cal BP (Table 1) coinciding with a MS maximum (839 cm) (Fig. 6). This suggests great variations in the abundance of magnetic minerals and rapid changes in sediment environmental magnetic characteristics. Therefore, MS fluctuation likely correlates with changes in the Al/Ti ratio, thus in the composition of the allochthonous and lithogenic sediment components, overprinted by syn- and postsedimentary redox changes, as suggested by a maximum of the Mn/Fe ratio ~10.9 ka cal BP (Fig. 6). LOI values generally show a downward curve although a

new maximum is documented ~10.94 ka cal BP (779 cm), synchronous to another maximum in the concentration of macrocharcoals (0.81 mm^2/g; Fig. 6). Overall, the comparison of the MS, LOI and XRF records (Fig. 6) suggests that the sediment section between 1330 and 785 cm likely corresponds to a change in the geomorphological configuration of the study area. The hydromorphic soils typical of a marshy environment that has predominated during the Younger Dryas, gave way to an alluvial plain environment during this phase of the early Holocene (Turu et al., 2018). From the results of geophysical surveys carried out in the Navamuño depression (Carrasco et al., 2015b, 2018), the sedimentary basin infill was produced by lateral accretion, on a meander-type pattern. Thus, the alluvial plain palaeogeography would have presented a flooded zone at the western edge, similar to the current situation, but deeper (Fig. 1). In contrast, the eastern part would have emerged to progress as a floodplain, where paleosols can be found (Turu et al., 2018), such as that dated at 785 cm depth (Table 2). This type of new configuration could explain that the initial contribution of sands came through the flows produced in the drainage channels of the basin, especially when these exceeded the floodplain. However, this sedimentary process stopped when there was no material supply and various successive sedimentation stages may have occurred, including the dominance of silts. At this time it is feasible to assume the total disappearance in the depression of any lake-type structure (Carrasco et al., 2018). Subsequently, the Navamuño depression seems to stabilize ~10.95–10.6 ka cal BP, reducing the sedimentation rate to 2.19 mm yr^{-1} (Fig. 2). This is followed by a stepwise decrease in LOI, MS, Al/Ti and Mn/Fe ratios (Fig. 6), suggesting higher and poorly oxygenated waters.

The reconstructed Pann and Tann values (Fig. 6) at the start of the late Preboreal ~11.3–11.1 ka cal BP clearly show an increase in both rainfall and temperature, with maximum values ~11.11 ka cal BP coinciding with the abovementioned maximum percentage of birch, indicanting wetter and warmer conditions. Later, Pann values show a downward trend until ~10.9 ka cal BP, while Tann progressively increases coinciding with a *Pinus sylvestris/nigra* peak, and therefore with a drier and warmer phase. This last phase is only briefly interrupted ~10.97 ka cal BP when Pann increases and Tann decreases. Here major sedimentary facies changes arise related to a less proximal alluvial-fan system (Turu et al., 2018). Subsequently, Pann values progressively increase until ~10.67 ka cal BP while Tann values decrease. Finally, both trends are reversed by increasing Tann and decreasing Pann values until ~10.6 ka cal BP, indicating a warmer and drier phase concomitant with the development of high-mountain pines, broom communities and cryoxerophytic taxa (Fig. 6). A similar trend is documented in the NGRIP core (Rasmussen et al., 2008) during the late Preboreal ~11.3–10.6 ka cal BP by a progressive increase in δ^{18}O values, although some minimum values are also documented by decreases in δ^{18}O values that are contemporary with the Tann decreases discussed above (Fig. 6). In short, the great climatic instability demonstrated by both the pollen record and the paleoclimatic reconstruction of Navamuño during the Preboreal are in agreement with similar research carried out in northern Europe (Björck et al., 1997; Bos et al., 2007) and the Iberian Peninsula (Tarroso et al., 2016; Ilvonen et al., 2019), as well as with most Iberian pollen records, especially those of the Mediterranean region (Carrión et al., 2010; Carrión, 2012) and particularly in inland areas where continentality played a fundamental role (Aranbarri et al., 2014), while those of the Eurosiberian region are more stable (Iriarte-Chiapusso et al., 2016).

6. Conclusions

High-resolution multiproxy analyses of the Navamuño record allow the reconstruction of vegetation and fire dynamics, climate and hydrological changes in the western ICS during the Late Glacial and the early Holocene (~15.6–10.6 ka cal BP). This core provides one of the few continental records of the entire Late Glacial-early Holocene periods in central Iberia showing the strongest vegetation changes yet published. Within this time frame, the Navamuño record exhibits a high temporal resolution in good agreement with the δ^{18}O oscillations documented at the NGRIP core (Rasmussen et al., 2008). Most of the studied period has been characterized by a marked resilience of terrestrial vegetation, particularly of high-mountain pine and birch woodlands, as well as by generally gradual responses to millennial and centennial-scale climate fluctuations. The main vegetation and hydrological responses to global climate variability have been identified using palynological, macrocharcoal and geochemical indicators, enabling correlations with other continental Iberian and southern Mediterranean palaeoenvironmental sequences (Watts et al., 1996; Carrión et al., 2010; González-Sampériz et al., 2010; Jalut et al., 2010; Carrión, 2012; Aranbarri et al., 2014; Iriarte-Chiapusso et al., 2016; Beaulieu et al., 2017; Sadori, 2018; Camuera et al., 2019). In general terms, ten phases occurred between ~15.6 and 10.6 ka cal BP as follows:

1) Regional cold and dry conditions are inferred for the Oldest Dryas stadial ~15.6–14.7 ka cal BP with high-mountain pine forests and cryoxerophytic elements as main landscape elements. In addition, the sedimentary facies reveal the presence of a glaciolacustrine depositional environment of an amictic lake at the beginning of the deglaciation.

2) Moister and warmer conditions characterize the Bølling sub-interstadial ~14.7–14.0 ka cal BP, showing the expansion of birch woodlands. In addition, the well-developed hydro-hygrophyte pollen and NPPs assemblages and the sedimentary facies associations reveal high water levels and oligotrophic open water conditions. However, a cooling phase is documented ~14.2–14.0 ka cal BP, coinciding with the development of high-mountain pine woodlands during the Intra-Bølling cold period.

3) Subsequently, new cold and arid conditions characterize the study area during the Older Dryas sub-interstadial ~14.0–13.4 ka cal BP, as demonstrated by the replacement of birch woodlands by high-mountain pines, broom communities and a steppe-like landscape dominated by xerophilous, heliophilous and cryophilous grasslands. Geochemical and sedimentary proxies suggest deeper and poorly oxygenated mixed water conditions in the palaeolake.

4) Prevalence of dry conditions in response to the warmer Greenland Interstadial 1c ~13.4–13.1 ka cal BP, when high-mountain pine woodlands and hydro-hygrophytes spread locally. Hydrologically, this phase corresponds with an oxygenated and oligotrophic environment under lower lake levels.

5) New moister conditions are recorded during the colder Intra-Allerød cold period ~13.1–12.9 ka cal BP in coherence with the progressive replacement of pine-dominated woodlands by mixed pine-birch woodlands, showing the expansion of cryoxerophytic and heliophilous/cryophilous elements. Local hydrological conditions suggest poorly oxygenated and meso-eutrophic water and higher lake levels.

6) The progressive increase in humid and warm conditions during the Allerød sub-interstadial ~12.9–12.6 ka cal BP enabled a rapid forest recolonization with the expansion of high-mountain pine forests and an overall low fire activity. Low lake levels and better oxygenated waters persisted during this period.

7) The Younger Dryas stadial ~12.6—11.7 ka cal BP worsening appears quite mitigated in the western ICS, showing a landscape dominated by open high-mountain pine forests and cold steppe grasslands with sparse riparian woodlands. Locally, sedimentary facies, palynological and geochemical proxyes point to lower and better oxygenated waters and the development of a marshy environment. From a climatic point of view, this period is characterized by a biphasic structure including dry and warm conditions ~12.6—12.0 ka cal BP and wetter and cooler ones ~12.0—11.7 ka cal BP.

8) The early Preboreal ~11.7—11.45 ka cal BP is expressed by a rapid temperature rise, which involved a rapid reforestation with high-mountain pines, broom communities and crawling junipers, and a dramatic reduction of riparian woodlands and open vegetation communities. The Navamuño depression was occupied by a shallow lagoon or more likely by a floodplain with stagnant shallow water. A great fire activity is attested at this time related to an increase in biomass availability.

9) The abrupt climate event ~11. 4 ka cal BP (Preboreal oscillation) is characterized by open mixed birch-pine woodlands and a dense shrub cover of broom, heather and crawling juniper ~11.45—11.3 ka cal BP. The dry and cool climate favored the development of cryophilous and xerophytic taxa and increased fire activity, while the increase of reed mat and Zygnemataceae suggest a shallow basin environment with dominant ephemeral meso-eutrophic lake conditions.

10) The late Preboreal ~11.3—10.6 ka cal BP is characterized by a highly variable climate, involving the antagonistic development of pine and birch forests, and the local expansion of deciduous oak woodlands. The great geomorphological change in the study area occurs in this period and can be correlated with the destabilization of the system after the 11.4 ka cal BP event. The Navamuño depression was transformed into a wide floodplain subject to the sedimentary flows of a meandriform system at the end.

Acknowledgements

References

Abel-Schaad, D., López-Sáez, J.A., 2013. Vegetation changes in relation to fire history and human activities at the Peña Negra mire (Béjar Range, Iberian Central Mountain System, Spain) during the past 4.000 years. Veg. Hist. Archaeobotany 22, 199—214. https://doi.org/10.1007/s00334-012-0368-9.

Abel-Schaad, D., Pulido, F.J., López-Sáez, J.A., Alba-Sánchez, F., Nieto-Lugilde, D., Franco-Múgica, F., Pérez-Díaz, S., Ruiz-Zapata, M.B., Gil-García, M.J., Dorado-Valiño, M., 2014. Persistence of tree relicts through the Holocene in the Spanish central system. Lazaroa 35, 107—131. https://doi.org/10.5209/rev_LAZA.2014.v35.41932.

Allen, J.R.M., Huntley, B., 2000. Weichselian palynological records from southern Europe: correlation and chronology. Quat. Int. 73/74, 111—125. https://doi.org/10.1016/S1040-6182(00)00068-9.

Alley, R., 2000. The Younger Dryas cold interval as viewed from central Greenland. Quat. Sci. Rev. 19, 213—226. https://doi.org/10.1016/S0277-3791(99)00062-1.

Ammann, B., Birks, H.H., Walanus, A., Wasylikowa, K., 2007. Plant macrofossil records - late glacial multidisciplinary studies. In: Elias, Scott A. (Ed.), Encyclopedia of Quaternary Science. Elsevier, Oxford, pp. 2475—2486.

Aranbarri, J., González-Sampériz, P., Valero-Garcés, B.L., Moreno, A., Gil-Romera, G., Sevilla, M., García-Prieto, E., di Rita, F., Mata, M.P., Morellón, M., Magri, D., Rodríguez-Lázaro, J., Carrión, J.S., 2014. Rapid climatic changes and resilient vegetation during the Lateglacial and Holocene in a continental region of southwestern Europe. Glob. Planet. Chang. 114, 50—65. https://doi.org/10.1016/j.gloplacha.2014.01.003.

Atienza, M., 1995. Estudio palinológico de los cambios en el límite superior del bosque durante el Holoceno en la Sierra de Béjar. Sistema Central Español. In: Aleixandre, T., Pérez, A. (Eds.), Reconstrucción de paleoambientes y cambios climáticos durante el Cuaternario. C.S.I.C., Madrid, pp. 329—338.

Atienza, M., Dorado, M., Gómez-Lobo, A., Ruiz-Zapata, M.B., 1996. Estudio polínico de un depósito situado en la vertiente norte de la Sierra de Béjar. Bot. Macaronés. 23, 201—209.

Baldini, L.M., McDermott, F., Baldini, J.U.L., Arias, P., Cueto, M., Fairchild, I.J., Hoffmann, D.L., Mattey, D.P., Müller, W., Nita, D.C., Ontañón, R., García-Moncó, C., Richards, D.A., 2015. Regional temperature, atmospheric circulation, and sea-ice variability within the Younger Dryas Event constrained using a speleothem from northern Iberia. Earth Planet. Sci. Lett. 419, 101—110. https://doi.org/10.1016/j.epsl.2015.03.015.

Bartolomé, M., Moreno, A., Sancho, C., Stoll, H.M., Cacho, I., Spötl, C., Belmonte, A., Edwards, R.L., Cheng, H., Hellstrom, J.C., 2015. Hydrological change in southern Europe responding to increasing north Atlantic overturning during Greenland stadial 1. Proc. Natl. Acad. Sci. 112, 6568—6572. https://doi.org/10.1073/pnas.1503990112.

Beaulieu, J.L. de, Brugiapaglia, E., Joannin, S., Guiter, F., Zanchetta, G., Wulf, S., Peyron, O., Bernardo, L., Didier, J., Stock, A., Rius, D., Magny, M., 2017. Lateglacial-Holocene abrupt vegetation changes at Lago Trifoglietti in Calabria, Southern Italy: the setting of ecosystems in a refugial zone. Quat. Sci. Rev. 158, 44—57. https://doi.org/10.1016/j.quascirev.2016.12.013.

Benito-Garzón, M., Sánchez de Dios, R., Sainz-Ollero, H., 2007. Predicitve modelling of tree species distributions on the iberian peninsula during the last glacial maximum and mid-holocene. Ecography 30, 120—134. https://doi.org/10.1111/j.0906-7590.2007.04813.x.

Benito-Garzón, M., Sánchez de Dios, R., Sainz-Ollero, H., 2008. Effects of climate change on the distribution of Iberian tree species. Appl. Veg. Sci. 11, 169—178. https://doi.org/10.3170/2008-7-18348.

Bennett, K.D., 1996. Determination of the number of zones in a biostratigraphical sequence. New Phytol. 132, 155—170. https://doi.org/10.1111/j.1469-8137.1996.tb04521.x.

Birks, H.J.B., Willis, K.J., 2008. Alpines, trees, and refugia in Europe. Plant Ecol. Divers. 1, 147—160. https://doi.org/10.1080/17550870802349146.

Birks, H.J.B., Heire, O., Seppä, H., Bjune, A.E., 2010. Strengths and weaknesses of quantitative climate reconstructions based on Late-Quaternary biological proxies. Open Ecol. J. 3, 68—110. https://doi.org/10.2174/1874213001003020068.

Björck, S., Rundgren, M., Ingólfsson, Ó., Funder, S., 1997. The Preboreal oscillation around the Nordic Seas: terrestrial and lacustrine responses. J. Quat. Sci. 12, 455—465. https://doi.org/10.1002/(SICI)1099-1417(199711/12)12:6<455::AID-JQS316>3.0.CO;2-S.

Blaauw, M., 2010. Methods and code for classical age-modelling of radiocarbon sequences. Quat. Geochronol. 5, 512—518. https://doi.org/10.1016/j.quageo.2010.01.002.

Bos, J.A.A., van Geel, B., van der Plicht, J., Bohncke, S.J.P., 2007. Preboreal climate oscillations in Europe: wiggle-match dating and synthesis of Dutch high-resolution multi-proxy records. Quat. Sci. Rev. 26 https://doi.org/10.1016/j.quascirev.2006.09.012, 1927—1950.

Brewer, S., Cheddadi, R., de Beaulieu, J.L., Reille, M., Data contributors, 2002. The spread of deciduous Quercus throughout Europe since the last glacial period. For. Ecol. Manag. 156, 27—48. https://doi.org/10.1016/S0378-1127(01)00646-6.

Broothaerts, N., Robles-López, S., Abel-Schaad, D., Pérez-Díaz, S., Alba-Sánchez, F., Luelmo-Lautenschlaeger, R., Glais, A., López-Sáez, J.A., 2018. Reconstructing past arboreal cover based on modern and fossil pollen data: a statistical approach for the Gredos Range (Central Spain). Rev. Palaeobot. Palynol. 255, 1—13. https://doi.org/10.1016/j.revpalbo.2018.04.007.

Burjachs, F., Expósito, I., 2015. Charcoal and pollen analysis: examples of Holocene fire dynamics in mediterranean iberian peninsula. Catena 135, 340—349. https://doi.org/10.1016/j.catena.2014.10.006.

Burjachs, F., Jones, S.E., Giralt, S., Fernández López de Pablo, J., 2016. Lateglacial to Early Holocene recursive aridity events in the SE Mediterranean Iberian Peninsula: the Salines playa lake case study. Quat. Int. 403, 187—200. https://doi.org/10.1016/j.quaint.2015.10.117.

Camarero, J.J., Sangüesa-Barreda, G., Montiel-Molina, C., Seijo, F., López-Sáez, J.A., 2018. Past growth suppressions as proxies of fire occurrence in relict Mediterranean black pine forests. For. Ecol. Manag. 413, 9—20. https://doi.org/10.1016/j.foreco.2018.01.046.

Camuera, J., Jiménez-Moreno, G., Ramos-Román, M.J., García-Alix, A., Toney, J.L., Scott Anderson, R., Jiménez-Espejo, F., Bright, J., Webster, C., Yanes, Y., Carrión, J.S., 2019. Vegetation and climate changes during the last two glacial-interglacial cycles in the western Mediterranean: a new long pollen record from Padul (southern Iberian Peninsula). Quat. Sci. Rev. 205, 86—105. https://doi.org/10.1016/j.quascirev.2018.12.013.

Camuera, J., Jiménez-Moreno, G., Ramos-Román, M.J., García-Alix, A., Toney, J.L., Scott Anderson, R., Jiménez-Espejo, F., Kaufman, D., Bright, J., Webster, C., Yanes, Y., Carrión, J.S., Ohkouchi, N., Suga, H., Yamame, M., Yokoyama, Y., Martínez-Ruiz, F., 2018. Orbital-scale environmental and climatic changes recorded in a new ~200,000-year-long multi-proxy sedimentary record from Padul,

southern Iberian Peninsula. Quat. Sci. Rev. 198, 91–114. https://doi.org/10.1016/j.quascirev.2018.08.014.

Carcaillet, C., Bergman, I., Delorme, S., Hornberg, G., Zackrisson, O., 2007. Long-term fire frequency not linked to prehistoric occupations in northern Swedish boreal forest. Ecology 88, 465–477. https://doi.org/10.1890/0012-9658(2007)88[465:LFFNLT]2.0.CO;2.

Carcaillet, C., Bouvier, M., Fréchette, B., Larouche, C., Richard, P.J.H., 2001. Comparison of pollen-slide and sieving methods in lacustrine charcoal analyses for local and regional fire history. Holocene 11, 467–476. https://doi.org/10.1191/095968301678302904.

Carrasco, R.M., 1997. Estudio geomorfológico del Valle del Jerte (Sistema Central Español): secuencia de procesos y dinámica morfogenética actual. Ph.D. Thesis. Complutense University of Madrid.

Carrasco, R.M., Pedraza, J., Domínguez-Villar, D., Villa, J., Willenbring, J.K., 2013. The plateau glacier in the Sierra de Béjar (Iberian Central System) during its maximum extent. Reconstruction and chronology. Geomorphology 196, 83–93. https://doi.org/10.1016/j.geomorph.2012.03.019.

Carrasco, R.M., Pedraza, J., Domínguez-Villar, D., Willenbring, J.K., Villa, J., 2015a. Sequence and chronology of the Cuerpo de Hombre paleoglacier (Iberian Central System) during the last glacial cycle. Quat. Sci. Rev. 129, 163–177. https://doi.org/10.1016/j.quascirev.2015.09.021.

Carrasco, R.M., Sánchez, J., Muñoz-Martín, A., Pedraza, J., Olaiz, A.J., Ruiz-Zapata, B., Abel-Schaad, D., Merlo, O., Domínguez-Villar, D., 2015b. Caracterización de la geometría de la depresión de Navamuño (Sistema Central Español) aplicando técnicas geofísicas. Geogaceta 57, 39–42.

Carrasco, R.M., Turu, V., Pedraza, J., Muñoz-Martín, A., Ros, X., Sánchez, J., Ruiz-Zapata, B., Olaiz, A.J., Herrero-Simón, A., 2018. Near surface geophysical analysis of the Navamuño depression (Sierra de Béjar, Iberian Central System): geometry, sedimentary infill and genetic implications of tectonic and glacial footprint. Geomorphology 315, 1–16. https://doi.org/10.1016/j.geomorph.2018.05.003.

Carrión, J.S., 2002. Patterns and processes of Late Quaternary environmental change in a montane region of southwestern Europe. Quat. Sci. Rev. 21, 2047–2066. https://doi.org/10.1016/S0277-3791(02)00010-0.

Carrión, J.S., Navarro, C., 2002. Cryptogam spores and other non-pollen microfossils as sources of palaeoecological information: case-studies from Spain. Ann. Bot. Fenn. 39, 1–14.

Carrión, J.S., (Coord.), 2012. Paleoflora y paleovegetación de la Península Ibérica e Islas Baleares: Plioceno-Cuaternario. Ministerio de Economía y Competitividad, Madrid.

Carrión, J.S., Fernández, S., González-Sampériz, P., Gil-Romera, G., Badal, E., Carrión, Y., López-Merino, L., López-Sáez, J.A., Fierro, E., Burjachs, F., 2010. Expected trends and surprises in the late glacial and Holocene vegetation history of the iberian peninsula and balearic islands. Rev. Palaeobot. Palynol. 162, 458–475. https://doi.org/10.1016/j.revpalbo.2009.12.007.

Carrión, J.S., Fernández, S., González-Sampériz, P., Leroy, S.A.G., Bailey, G.N., López-Sáez, J.A., Burjachs, F., Gil-Romera, G., García-Antón, M., Gil-García, M.J., Parra, I., Santos, L., López-García, P., Yll, E.I., Dupré, M., 2009. Quaternary pollen analysis in the Iberian Peninsula: the value of negative results. Internet Archaeol. 25, 1–53. https://doi.org/10.11141/ia.25.5.

Carrión, J.S., Navarro, C., Navarro, J., Munuera, M., 2000. The distribution of cluster pine (Pinus pinaster) in Spain as derived from palaeoecological data, relationships with phytosociological classification. Holocene 10, 243–252. https://doi.org/10.1191/095968300676937462.

Casas-Sainz, A.M., de Vicente, G., 2009. On the tectonic origin of Iberian topography. Tectonophysics 474, 214–235. https://doi.org/10.1016/j.tecto.2009.01.030.

Chesworth, W., Martínez-Cortizas, A., García-Rodeja, E., 2006. Redox-pH approach to the geochemistry of the Earth's land surface, with application to peatlands. In: Martini, I.P., Martínez-Cortizas, A., Chesworth, W. (Eds.), Peatlands: Evolution and Records of Environmental and Climate Changes. Elsevier, Amsterdam, pp. 175–196.

Cohen, A.S., 2003. Paleolimnology: the History and Evolution of Lake Systems. Oxford University Press, New York.

Comes, H.P., Kadereit, J.W., 1998. The effect of Quaternary climatic changes on plant distribution and evolution. Trends Plant Sci. 3, 432–438. https://doi.org/10.1016/S1360-1385(98)01327-2.

Connor, S.E., Araújo, J., van der Knapp, W.O., van Leeuwen, J.F.N., 2012. A long-term perspective on biomass burning in the Serra da Estrela, Portugal. Quat. Sci. Rev. 55, 114–124. https://doi.org/10.1016/j.quascirev.2012.08.007.

Connor, S.E., Vannière, B., Colombaroli, D., Scott Anderson, R., Carrión, J.S., Ejarque, A., Gil-Romera, G., González-Sampériz, P., Hoefer, D., Morales-Molino, C., Revelles, J., Schneider, H., van der Knaap, W.O., van Leeuwen, J.F.N., Woodbridge, J., 2019. Humans take control of fire-driven diversity changes in Mediterranean Iberia's vegetation during the mid-late Holocene. Holocene 29, 886–901. https://doi.org/10.1177/0959683619826652.

Cugny, C., Mazier, F., Galop, D., 2010. Modern and fossil non-pollen palynomorphs from the Basque mountains (western Pyrenees, France): the use of coprophilous fungi to reconstruct pastoral activity. Veg. Hist. Archaeobotany 19, 391–408. https://doi.org/10.1007/s00334-010-0242-6.

Daniau, A.L., Sánchez-Goñi, M.F., Beaufort, L., Laggoun-Défarge, F., Loutre, M.F., Duprat, J., 2007. Dansgaard-Oeschger climatic variability revealed by fire emissions in southwestern Iberia. Quat. Sci. Rev. 26, 1369–1383. https://doi.org/10.1016/j.quascirev.2007.02.005.

Davis, B.A.S., Zanon, M., Collins, P., Mauri, A., Bakker, J., Barboni, D., Barthelmes, A., Beaudouin, C., Birks, H.J.B., Bjune, A.E., Bozilova, E., Bradshaw, R.H.W.,

Brayshay, B.A., Brewer, S., Brugiapaglia, E., Bunting, J., Connor, S.E., de Beaulieu, J.L., Edwards, K.J., Ejarque, A., Fall, P., Florenzano, A., Fyfe, R., Galop, D., Giardini, M., Giesecke, T., Grant, M.J., Guiot, J., Jahns, S., Jankovská, V., Juggins, S., Kahrmann, M., Karpińska-Kołaczek, M., Kołaczek, P., Kühl, N., Kuneš, P., Lapteva, E.G., Leroy, S.A.G., Leydet, M., López-Sáez, J.A., Masi, A., Matthias, I., Mazier, F., Meltsov, V., Mercuri, A.M., Miras, Y., Mitchell, F.J.G., Morris, J.L., Naughton, F., Nielsen, A.B., Novenko, E., Odgaard, B., Ortu, E., Overballe-Petersen, M.V., Pardoe, H.S., Peglar, S.M., Pidek, I.A., Sadori, L., Seppä, H., Severova, E., Shaw, H., Święta-Musznicka, J., Theuerkauf, M., Tonkov, S., Veski, S., van der Knaap, P.W.O., van Leeuwen, J.F.N., Woodbridge, J., Zimny, M., Kaplan, J.O., 2013. The European modern pollen database (EMPD) project. Veg. Hist. Archaeobotany 22, 521–530. https://doi.org/10.1007/s00334-012-0388-5.

Davison, W., 1993. Iron and manganese in lakes. Earth Sci. Rev. 34, 119–163. https://doi.org/10.1016/0012-8252(93)90029-7.

Demory, F., Oberhansli, H., Nowaczyk, N.R., Gottschalk, M., Wirth, R., Naumann, R., 2005. Detrital input of early diagenesis in sediments from Lake Baikal revealed by rock magnetism. Glob. Planet. Chang. 46, 145–166. https://doi.org/10.1016/j.gloplacha.2004.11.010.

Denton, G.H., Broecker, W.S., Alley, R.B., 2006. The mystery interval 17.5 to 14.5 kyrs ago. PAGES News 14, 14–16. https://doi.org/10.22498/pages.14.2.14.

Desprat, S., Díaz-Fernández, P., Coulon, T., Ezzat, L., Pessarossi-Langlois, J., Gil, L., Morales-Molino, C., Sánchez Goñi, M.F., 2015. Pinus nigra (Spanish black pine) as the dominant species of the last glacial pinewoods in south-western to central Iberia: a morphological study of modern and fossil pollen. J. Biogeogr. 42, 1998–2009. https://doi.org/10.1111/jbi.12566.

Domínguez-Villar, D., Carrasco, R.M., Pedraza, J., Cheng, H., Edwards, R.L., Willenbring, J.K., 2013. Early maximum extent of paleoglaciers from Mediterranean mountains during the last glaciation. Sci. Rep. 3 (2034), 1–6. https://doi.org/10.1038/srep02034.

Drescher-Schneider, R., Beaulieu, J.L. de, Magny, M., Walter-Simonnet, A.V., Bossuet, G., Millet, L., Brugiapaglia, E., Drescher, A., 2007. Vegetation history, climate and human impact over the last 15,000 years at Lago dell'Accesa (Tuscany, Central Italy). Veg. Hist. Archaeobotany 16, 279–299. https://doi.org/10.1007/s00334-006-0089-z.

Feurdean, A., Spessa, A., Magyari, E.K., Willis, K.J., Veres, D., Hickler, T., 2012. Trends in biomass burning in the Carpathian region over the last 15,000 years. Quat. Sci. Rev. 45, 111–125. https://doi.org/10.1016/j.quascirev.2012.04.001.

Fick, S.E., Hijmans, R.J., 2017. Worldclim 2: new 1-km spatial resolution climate surfaces for global land areas. Int. J. Climatol. 37, 4302–4315. https://doi.org/10.1002/joc.5086.

Finsinger, W., Kelly, R., Fevre, J., Magyari, E.K., 2014. A guide to screening charcoal peaks in macrocharcoal-area records for fire-episode reconstructions. Holocene 24, 1002–1008. https://doi.org/10.1177/0959683614534737.

Fisher, T.G., Smith, D.G., Andrews, J.T., 2002. Preboreal oscillation caused by a glacial Lake Agassiz flood. Quat. Sci. Rev. 21, 873–878. https://doi.org/10.1016/S0277-3791(01)00148-2.

Fletcher, W.J., Sánchez-Goñi, M.F., Allen, J.R.M., Cheddadi, R., Cambourieu-Nebout, N., Huntley, B., Lawson, I., Londeix, L., Magri, D., Margari, V., Muller, U.C., Naughton, F., Novenko, E., Roucoux, K., Tzedakis, P.C., 2010. Millennial-scale variability during the last glacial in vegetation records from Europe. Quat. Sci. Rev. 29, 2839–2864. https://doi.org/10.1016/j.quascirev.2009.11.015.

Gaillard, M.J., Sugita, S., Bunting, J., Middleton, R., Brostrom, A., Caseldine, C., Giesecke, T., Hellman, S.E.V., Hicks, S., Hjelle, K., Langdon, C., Nielsen, A.B., Poska, A., vonStedingk, H., Veski, S., POLLANDCAL members, 2008. The use of modelling and simulation approach in reconstructing past landscapes from fossil pollen data: areview and results from the POLLANDCAL network. Veg. Hist. Archaeobotany 17, 419–443. https://doi.org/10.1007/s00334-008-0169-3.

García-Alix, A., Jiménez-Moreno, G., Jiménez-Espejo, F.J., García-García, F., Delgado Huertas, A., 2014. An environmental snapshot of the Bølling interstadial in Southern Iberia. Quat. Res. 81, 284–294. https://doi.org/10.1016/j.yqres.2014.01.009.

García-Álvarez, S., Bal, M.C., Allée, P., García-Amorena, I., Rubiales, J.M., 2017. Holocene treeline history of a high-mountain landscape inferred from soil charcoal: the case of Sierra de Gredos (Iberian Central Sytem, SW Europe). Quat. Int. 457, 85–98. https://doi.org/10.1016/j.quaint.2017.04.019.

García-Amorena, I., Rubiales, J.M., Moreno-Amat, E., Iglesias, R., Gómez-Manzaneque, F., 2011. New macrofossil evidence of Pinus nigra arnold on the northern iberian meseta during the Holocene. Rev. Palaeobot. Palynol. 163, 281–288. https://doi.org/10.1016/j.revpalbo.2010.10.010.

García-Ruiz, J.M., Palacios, D., González-Sampériz, P., de Andrés, N., Moreno, A., Valero-Garcés, B., Gómez-Villar, A., 2016. Mountain glacier evolution in the iberian peninsula during the younger Dryas. Quat. Sci. Rev. 138, 26–30. https://doi.org/10.1016/j.quascirev.2016.02.022.

Gavilán, R., 2005. The use of climatic parameters and indices in vegetation distribution. A case study in the Spanish Sistema Central. Int. J. Biometeorol. 50, 111–120. https://doi.org/10.1007/s00484-005-0271-5.

GEODE, 2004. Cartografía geológica digital contínua a escala 1:50.000 del Instituto Geológico y Minero de España. http://info.igme.es/cartografiadigital/geologica/Geode.aspx. (Accessed 7 February 2019).

Giesecke, T., Brewer, S., Finsinger, W., Leydet, M., Bradshaw, R.H.W., 2017. Patterns and abundance of European vegetation change over the last 15,000 years. J. Biogeogr. 44, 1441–1456. https://doi.org/10.1111/jbi.12974.

Gil-Romera, G., Carrión, J.S., Pausas, J.G., Sevilla, M., Lamb, H.J., Fernández, S., Burjachs, F., 2010a. Holocene fire activity and vegetation response in South-Eastern Iberia. Quat. Sci. Rev. 29, 1082–1092. https://doi.org/10.1016/

j.quascirev.2010.01.006.

Gil-Romera, G., González-Sampériz, P., Lasheras-Álvarez, L., Sevilla-Callejo, M., Moreno, A., Valero-Garcés, B., López-Merino, L., Carrión, J.S., Pérez-Sanz, A., Aranbarri, J., García-Prieto, E., 2014. Biomass-modulated fire dynamics during the last glacial-interglacial transition at the central Pyrenees (Spain). Palaeogeogr. Palaeoclimatol. Palaeoecol. 402, 113–124. https://doi.org/10.1016/j.palaeo.2014.03.015.

Gil-Romera, G., López-Merino, L., Carrión, J.S., González-Sampériz, P., Martín-Puertas, C., López-Sáez, J.A., Fernández, S., García-Antón, M., Stefanova, V., 2010b. Interpreting resilience through long-term ecology: potential insights in Western Mediterranean landscapes. Open Ecol. J. 3, 43–53. https://doi.org/10.2174/1874213001003020043.

González-Sampériz, P., Leroy, S.A.G., Carrión, J.S., Fernández, S., García-Antón, M., Gil-García, M.J., Uzquiano, P., Valero-Garcés, B., Figueiral, I., 2010. Steppes, savannahs, forests and phytodiversity reservoirs during the Pleistocene in the Iberian Peninsula. Rev. Palaeobot. Palynol. 162, 427–457. https://doi.org/10.1016/j.revpalbo.2010.03.009.

González-Sampériz, P., Valero-Garcés, B.L., Moreno, A., Jalut, G., García-Ruiz, J.M., Martí-Bono, C.E., Delgado-Huertas, A., Navas, A., Otto, T., Dedoubat, J.J., 2006. Climate variability in the Spanish Pyrenees during the last 30,000 yr revealed by the El Portalet sequence. Quat. Res. 66, 38–52. https://doi.org/10.1016/j.yqres.2006.02.004.

Grimm, E.C., 1987. Coniss: a Fortran 77 program for stratigraphically constrained cluster analysis by the method of incremental sum of squares. Comput. Geosci. 13, 13–35. https://doi.org/10.1016/0098-3004(87)90022-7.

Grimm, E.D., 2004. TGView. Illinois State Museum. Research and Collection Center, Springfield.

Guiot, J., 1990. Methodology of the last climatic cycle reconstruction in France from pollen data. Palaeogeogr. Palaeoclimatol. Palaeoecol. 80, 49–69. https://doi.org/10.1016/0031-0182(90)90033-4.

Haliuc, A., Veres, D., Brauer, A., Hubay, K., Hutchinson, S.M., Begy, R., Braun, M., 2017. Palaeohydrological changes during the mid and late Holocene in the Carpathian area, central-eastern Europe. Glob. Planet. Chang. 152, 99–114. https://doi.org/10.1016/j.gloplacha.2017.02.010.

Harrison, S.P., Prentice, C.I., 2003. Climate and CO_2 controls on global vegetation distribution at the last glacial maximum: analysis based on paleovegetation data, biome modeling and paleoclimate simulations. Glob. Chang. Biol. 9, 983–1004. https://doi.org/10.1046/j.1365-2486.2003.00640.x.

Heiri, O., Lotter, A.F., Lemacke, G., 2001. Loss-on-ignition for estimating organic and carbonate content in sediments: reproducibility and comparability of results. J. Paleolimnol. 25, 101–110. https://doi.org/10.1023/A:1008119611481.

Hernández-Díaz, J.M., Avilés-Amat, A., 2013. Historia de Béjar. Diputación Provincial de Salamanca, Salamanca.

Hewitt, G.M., 1999. Post-glacial re-colonization of European biota. Biol. J. Linn. Soc. 68, 87–112. https://doi.org/10.1006/bijl.1999.0332.

Hewitt, G.M., 2000. The genetic legacy of the Quaternary ice ages. Nature 405, 907–913. https://doi.org/10.1038/35016000.

Höobig, N., Weber, M.E., Kehl, M., Weniger, G.C., Julià, R., Melles, M., Fülöop, R.H., Vogel, H., Reicherter, K., 2012. Lake Banyoles (northeastern Spain): a Last Glacial to Holocene multi-proxy study with regard to environmental variability and human occupation. Quat. Int. 274, 205–218. https://doi.org/10.1016/j.quaint.2012.05.036.

Huntley, B., 1990. European vegetation history: palaeovegetation maps from pollen data - 13.000 yr. BP to present. J. Quat. Sci. 5, 103–122. https://doi.org/10.1002/jqs.3390050203.

Ilvonen, L., López-Sáez, J.A., Holmström, L., Alba-Sánchez, F., Pérez-Díaz, S., Carrión, J.S., Seppä, H., 2019. Quantitative reconstruction of precipitation changes in the iberian peninsula during the late Pleistocene and the Holocene. Clim. Past Discuss. https://doi.org/10.5194/cp-2019-33.

Iriarte-Chiapusso, M.J., Muñoz-Sobrino, C., Gómez-Orellana, L., Hernández-Beloqui, B., García-Moreiras, I., Fernández-Rodríguez, C., Heiri, O., Lotter, A.F., Ramil-Rego, P., 2016. Reviewing the Lateglacial-Holocene transition in NW Iberia: a palaeoecological approach based on the comparison between dissimilar regions. Quat. Int. 403, 211–236. https://doi.org/10.1016/j.quaint.2015.09.029.

Jalut, G., Turu, V., Dedoubat, J.J., Otto, T., Ezquerra, J., Fontugne, M., Belet, J.M., Bonnet, L., de Celis, A.G., Redondo-Vega, J.M., Vidal-Romaní, J.R., Santos, L., 2010. Palaeoenvironmental studies in NW Iberia (Cantabrian range): vegetation history and synthetic approach of the last deglaciation phases in the western Mediterranean. Palaeogeogr. Palaeoclimatol. Palaeoecol. 297, 330–350. https://doi.org/10.1016/j.palaeo.2010.08.012.

Juggins, S., 2007. User Guide C2. Sofware for Ecological and Paleoecological Data Analysis and Visualization. University of Newcastle, Newcastle.

Koinig, K., Shotyk, W., Lotter, A., Ohlendorf, C., 2003. 9000 years of geochemical evolution of lithogenic major and trace elements in the sediment of an alpine lake. J. Paleolimnol. 4, 307–320. https://doi.org/10.1023/A:1026080712312.

Kylander, M.E., Ampel, L., Wohlfarth, B., Veres, D., 2011. High-resolution X-ray fluorescence core scanning analysis of Les Echets (France) sedimentary sequence: new insights from chemical proxies. J. Quat. Sci. 26, 109–117. https://doi.org/10.1002/jqs.1438.

López, P., Navarro, E., Marce, R., Ordóñez, J., Caputo, L., Armengol, J., 2006. Elemental ratios in sediments as indicators of ecological processes in Spanish reservoirs. Limnética 25, 499–512.

López-Merino, L., López-Sáez, J.A., Ruiz-Zapata, M.B., Gil-García, M.J., 2008. Reconstructing the history of beech (Fagus sylvatica L.) in north-western Iberian

Range (Spain): from Late-Glacial refugia to Holocene anthropic induced forests. Rev. Palaeobot. Palynol. 152, 58–65. https://doi.org/10.1016/j.revpalbo.2008.04.003.

López-Merino, L., Silva-Sánchez, N., Kaal, J., López-Sáez, J.A., Martínez-Cortizas, A., 2012. Post-disturbance vegetation dynamics during the late Pleistocene and the Holocene: an example from NW Iberia. Glob. Planet. Chang. 92–93, 58–70. https://doi.org/10.1016/j.gloplacha.2012.04.003.

López-Sáez, J.A., 1993. Las alisedas (Scrophulario-Alnetum glutinosae) del Valle del Tiétar (Sierra de Gredos, Ávila): estado de conservación y presencia de especies relícticas del Terciario y Pliocuaternario. In: Silva, F.J., Vega, G. (Eds.), I Congreso Forestal Español, vol. IV. S.F.E., Pontevedra, pp. 41–46.

López-Sáez, J.A., López-García, P., 1994. Contribution of the palaeoecological knowledge of quaternary in the tietar valley (Sierra de Gredos, ávila, Spain). Rev. Espanola Micropaleontol. 26, 61–66.

López-Sáez, J.A., López Merino, L., 2007. Coprophilous fungi as a source of information of anthropic activities during the Prehistory in the Amblés Valley (Ávila, Spain): the archaeopalynological record. Rev. Espanola Micropaleontol. 39, 103–116.

López-Sáez, J.A., Abel-Schaad, D., Luelmo-Lautenschlaeger, R., Robles-López, S., Pérez-Díaz, S., Alba-Sánchez, F., Sánchez-Mata, D., Gavilán, R.G., 2018a. Resilience, vulnerability and conservation strategies in high-mountain pine forests in the Gredos range, central Spain. Plant Ecol. Divers. 11, 97–110. https://doi.org/10.1080/17550874.2018.1449261.

López-Sáez, J.A., Abel-Schaad, D., Pérez-Díaz, S., Blanco-González, A., Alba-Sánchez, F., Dorado, M., Ruiz-Zapata, B., Gil-García, M.J., Gómez-González, C., Franco-Múgica, F., 2014. Vegetation history, climate and human impact in the Spanish Central System over the last 9,000 years. Quat. Int. 353, 98–122. https://doi.org/10.1016/j.quaint.2013.06.034.

López-Sáez, J.A., Alba-Sánchez, F., López-Merino, L., Pérez-Díaz, S., 2010a. Modern pollen analysis: a reliable tool for discriminating Quercus rotundifolia communities in Central Spain. Phytocoenologia 40, 57–72. https://doi.org/10.1127/0340-269X/2010/0040-0430.

López-Sáez, J.A., Alba-Sánchez, F., Sánchez-Mata, D., Abel-Schaad, D., Gavilán, R.G., Pérez-Díaz, S., 2015. A palynological approach to the study of Quercus pyrenaica forest communities in the Spanish Central System. Phytocoenologia 45, 107–124. https://doi.org/10.1127/0340-269X/2014/0044-0572.

López-Sáez, J.A., Alba-Sánchez, F., Sánchez-Mata, D., Luengo-Nicolau, E., 2019. Los pinares de la Sierra de Gredos. Pasado, presente y futuro. Institución Gran Duque de Alba, Ávila.

López-Sáez, J.A., Glais, A., Robles-López, S., Alba-Sánchez, F., Pérez-Díaz, S., Abel-Schaad, D., Luelmo-Lautenschlaeger, R., 2017. Unraveling the naturalness of sweet chestnut forests (Castanea sativa Mill.) in central Spain. Veg. Hist. Archaeobotany 26, 167–182. https://doi.org/10.1007/s00334-016-0575-x.

López-Sáez, J.A., López-Merino, L., Alba-Sánchez, F., Pérez-Díaz, S., Abel-Schaad, D., Carrión, J.S., 2010b. Late Holocene ecological history of Pinus pinaster forests in the Sierra de Gredos of central Spain. Plant Ecol. 206, 195–209. https://doi.org/10.1007/s11258-009-9634-z.

López-Sáez, J.A., Sánchez-Mata, D., Alba-Sánchez, F., Abel-Schaad, D., Gavilán, R., Pérez-Díaz, S., 2013. Discrimination of Scots pine forests in the Iberian Central System (Pinus sylvestris var. iberica) by means of pollen analysis. Phytosociological considerations. Lazaroa 34, 191–208. https://doi.org/10.5209/rev_LAZA.2013.v34.n1.43599.

López-Sáez, J.A., Sánchez-Mata, D., Gavilán, R.G., 2016. Syntaxonomical update on the relict groves of Scots pine (Pinus sylvestris L. var. iberica Svoboda) and Spanish black pine (Pinus nigra Arnold subsp. salzmannii (Dunal) Franco) in the Gredos range (central Spain). Lazaroa 37, 153–172. https://doi.org/10.5209/LAZA.54043.

López-Sáez, J.A., van Geel, B., Farbos-Texier, S., Diot, M.F., 1998. Remarques paléoécologiques à propos de quelques palynomorphes non-polliniques provenant de sédiments quaternaires en France. Rev. Paléobiol. 17, 445–459.

López-Sáez, J.A., Vargas, G., Ruiz, J., Blarquez, O., Alba-Sánchez, F., Oliva, M., Pérez-Díaz, S., Robles-López, S., Abel-Schaad, D., 2018b. Paleofire dynamics in central Spain during the late Holocene: the role of climatic and anthropogenic forcing. Land Degrad. Dev. 29, 2045–2059. https://doi.org/10.1002/ldr.2751.

Lowe, J.J., Rasmussen, S.O., Björck, S., Hoek, W.Z., Steffensen, J.P., Walker, M.J.C., Yu, Z.C., 2008. Synchronisation of palaeoenvironmental events in the North Atlantic region during the Last Termination: a revised protocol recommended by the INTIMATE group. Quat. Sci. Rev. 27, 6–17. https://doi.org/10.1016/j.quascirev.2007.09.016.

Luceño, M., Vargas, P., 1991. In: Guía Botánica del Sistema Central Español. Pirámide, Madrid.

Magri, D., Di Rita, F., Aranbarri, J., Fletcher, W., González-Sampériz, P., 2017. Quaternary disappearance of tree taxa from Southern Europe: timing and trends. Quat. Sci. Rev. 163, 23–55. https://doi.org/10.1016/j.quascirev.2017.02.014.

Markgraf, V., 1980. Pollen dispersal in a mountain area. Grana 19, 127–146. https://doi.org/10.1080/00173138009424995.

Marlon, J.R., Bartlein, P.J., Walsh, M.K., Harrison, S.P., Brown, K.J., Edwards, M.E., Higuera, P.E., Power, M.J., Anderson, R.S., Briles, C., Brunelle, A., Carcaillet, C., Daniels, M., Hu, F.S., Lavoie, M., Long, C., Minckley, T., Richard, P.J.H., Scott, A.C., Shafer, D.S., Tinner, W., Umbanhowar, C.E., Whitlock, C., 2009. Wildfire responses to abrupt climate change in North America. Proc. Natl. Acad. Sci. U.S.A. 106, 2519–2524. https://doi.org/10.1073/pnas.0808212106.

Martín-Puertas, C., Jiménez-Espejo, F., Martínez-Ruiz, F., Nieto-Moreno, V., Rodrigo, M., Mata, M.P., Valero-Garcés, B.L., 2011. Late Holocene climate variability in the southwestern Mediterranean region: an integrated marine and

terrestrial geochemical approach. Clim. Past 6, 807–816. https://doi.org/10.5194/cp-6-807-2010.

Mateus, J.E., 1989. Pollen morphology of Portuguese ericales. Rev. Biol. 14, 135–208.

Mesa-Fernández, J.M., Jiménez-Moreno, G., Rodrigo-Gámiz, M., García-Alix, A., Jiménez-Espejo, F.J., Martínez-Ruiz, F., Anderson, R.S., Camuera, J., Ramos-Román, M.J., 2018. Vegetation and geochemical responses to Holocene rapid climate change in the Sierra Nevada (southeastern Iberia): the Laguna Hondera record. Clim. Past 14, 1687–1706. https://doi.org/10.5194/cp-14-1687-2018.

Miola, A., 2012. Tools for Non-Pollen Palynomorphs (NPPs) analysis: a list of Quaternary NPP types and reference literature in English language (1972-2011). Rev. Palaeobot. Palynol. 186, 142–161. https://doi.org/10.1016/j.revpalbo.2012.06.010.

Moore, P.D., Webb, J.A., Collinson, M.E., 1991. Pollen Analysis. Blackwell, London.

Morales-Molino, C., García-Antón, M., 2014. Vegetation and fire history since the last glacial maximum in an inland area of the western Mediterranean Basin (Northern Iberian Plateau, NW Spain). Quat. Res. 81, 63–77. https://doi.org/10.1016/j.yqres.2013.10.010.

Morales-Molino, C., García-Antón, M., Postigo-Mijarra, J.M., Morla, C., 2013. Holocene vegetation, fire and climate interactions on the westernmost fringe of the Mediterranean Basin. Quat. Sci. Rev. 59, 5–17. https://doi.org/10.1016/j.quascirev.2012.10.027.

Morellón, M., Aranbarri, J., Moreno, A., González-Sampériz, P., Valero-Garcés, B.L., 2018. Early Holocene humidity patterns in the Iberian Peninsula reconstructed from lake, pollen and speleothem records. Quat. Sci. Rev. 181, 1–18. https://doi.org/10.1016/j.quascirev.2017.11.016.

Morellón, M., Valero-Garcés, B., Vegas-Villarrúbia, T., González-Sampériz, P., Romero, O., Delgado-Huertas, A., Mata, P., Moreno, A., Rico, M., Corella, J.P., 2009. Lateglacial and Holocene palaeohydrology in the western mediterranean región: the lake estanya record (NE Spain). Quat. Sci. Rev. 28, 2582–2599. https://doi.org/10.1016/j.quascirev.2009.05.014.

Moreno, A., López-Merino, L., Leira, M., Marco-Barba, J., González Sampériz, P., Valero Garcés, B., López-Sáez, J.A., Santos, L., Mata, P., Ito, E., 2011. Revealing the last 13,500 years of environmental history from the multiproxy record of a mountain lake (Lago Enol, northern Iberian Peninsula). J. Paleolimnol. 46, 327–349. https://doi.org/10.1007/s10933-009-9387-7.

Moreno, A., Svensson, A., Brooks, S.K., Connor, S., Engels, S., Fletcher, W., Genty, D., Heiri, O., Labuhn, I., Persoiu, A., Peyron, O., Sadori, L., Valero-Garcés, B.L., Wulf, S., Zanchetta, G., 2014. A compilation of western European terrestrial records 60-8 ka BP: towards an understanding of latitudinal climatic gradients. Quat. Sci. Rev. 106, 167–185. https://doi.org/10.1016/j.quascirev.2014.06.030.

Moreno-Rodríguez, J.M., Viedma, O., Zavala, G., Luna, B., 2011. Landscape variables influencing forest fires in central Spain. Int. J. Wildland Fire 20, 678–689. https://doi.org/10.1071/WF10005.

Muñoz-Sobrino, C., Heiri, O., Hazekamp, M., van der Velden, D., Kirilova, E.P., García-Moreiras, I., Lotter, A.F., 2013. New data on the Lateglacial period of SW Europe: a high resolution multiproxy record from Laguna de la Roya (NW Iberia). Quat. Sci. Rev. 80, 58–77. https://doi.org/10.1016/j.quascirev.2013.08.016.

Muñoz-Sobrino, C., Ramil-Rego, P., Gómez-Orellana, L., 2004. Vegetation of the Lago de Sanabria area (NW Iberia) since the end of the Pleistocene: a palaeoecological reconstruction on the basis of two new pollen sequences. Veg. Hist. Archaeobotany 13, 1–22. https://doi.org/10.1007/s00334-003-0028-1.

Naeher, S., Gilli, A., North, R.P., Hamann, Y., Schubert, C.J., 2013. Tracing bottom water oxygenation with sedimentary Mn/Fe ratios in Lake Zurich, Switzerland. Chem. Geol. 352, 125–133. https://doi.org/10.1016/j.chemgeo.2013.06.006.

Naughton, F., Costas, S., Gomes, S.D., Desprat, S., Rodrigues, T., Sánchez-Goñi, M.F., Renssen, H., Trigo, R., Bronk-Ramsey, C., Oliveira, D., Salgueiro, E., Voelker, A.H.L., Abrantes, F., 2019. Coupled ocean and atmospheric changes during Greenland stadial 1 in southwestern Europe. Quat. Sci. Rev. 212, 108–120. https://doi.org/10.1016/j.quascirev.2019.03.033.

Naughton, F., Sanchez-Goñi, M.F., Desprat, S., Turon, J.L., Duprat, J., Malaize, B., Joli, C., Cortijo, E., Drago, T., Freitas, M.C., 2007. Present-day and past (last 25 000 years) marine pollen signal off Western Iberia. Mar. Micropaleontol. 62, 91–114. https://doi.org/10.1016/j.marmicro.2006.07.006.

Oliva-Urcía, B., Moreno, A., Leunda, M., Valero-Garcés, B.L., González-Sampériz, P., Gil-Romera, G., Mata, P., HORDA Group, 2018. Last deglaciation and Holocene environmental change at high altitude in the Pyrenees: the geochemical and paleomagnetic record from Marboré Lake (N Spain). J. Paleolimnol. 59, 349–371. https://doi.org/10.1007/s10933-017-0013-9.

Palacios, D., de Andrés, N., Gómez-Ortiz, A., García-Ruiz, J.M., 2016. Evidence of glacial activity during the Oldest Dryas in the mountains of Spain. In: Hughes, P.M., Woodward, J.C. (Eds.), Quaternary Glaciation in the Mediterranean Mountains, vol. 433. Geological Society Special Publications, London, pp. 87–110.

Palacios, D., Marcos, J., Vázquez-Selem, L., 2011. Last glacial maximum and deglaciation of Sierra de Gredos, central iberian peninsula. Quat. Int. 233, 16–26. https://doi.org/10.1016/j.quaint.2010.04.029.

Pals, J.P., van Geel, B., Delfos, A., 1980. Palaeoecological studies in the Klokkeweel bog near Hoogkarspel (prov of Noord-Holland). Rev. Palaeobot. Palynol. 30, 371–418. https://doi.org/10.1016/0034-6667(80)90020-2.

Pedraza, J., 1989. La morfogénesis del Sistema Central y su relación con la morfología granítica. Cad. Lab. Xeol. Laxe 13, 31–46.

Pedraza, J., 1994. Geomorfología del Sistema Central. In: Gutiérrez-Elorza, M. (Ed.), Geomorfología de España. Editorial Rueda, Madrid, pp. 63–100.

Pedraza, J., Carrasco, R.M., Domínguez-Villar, D., Villa, J., 2013. Late Pleistocene glacial evolutionary stages in the Gredos mountains (iberian central system).

Quat. Int. 302, 88–100. https://doi.org/10.1016/j.quaint.2012.10.038.

Peyron, O., Bégeot, C., Brewer, S., Heiri, O., Magny, M., Millet, L., Ruffaldi, P., Van Campo, E., Yu, G., 2005. Late-Glacial climatic changes in Eastern France (Lake Lautrey) from pollen, lake-levels, and chironomids. Quat. Res. 64, 197–211. https://doi.org/10.1016/j.yqres.2005.01.006.

Pons, A., Reille, M., 1988. The Holocene and upper Pleistocene pollen record from padul (granada, Spain): a new study. Palaeogeogr. Palaeoclimatol. Palaeoecol. 66, 243–263. https://doi.org/10.1016/0031-0182(88)90202-7.

Pontevedra, X., Castro, D., Carballeira, R., Souto, M., López-Sáez, J.A., Pérez-Díaz, S., Fraga, M.I., Valcárcel, M., García-Rodeja, E., 2017. Iberian acid peatlands: types, origin and general trends of development. Mires Peat 19, 1–19. https://doi.org/10.19189/MaP.2016.OMB.260.

Postigo-Mijarra, J.M., Gómez-Manzaneque, F., Morla, C., 2008. Survival and long-term maintenance of tertiary trees in the iberian peninsula during the Pleistocene: first record of aesculus L. (Hippocastanaceae) in Spain. Veg. Hist. Archaeobotany 17, 351–364. https://doi.org/10.1007/s00334-007-0130-x.

Postigo-Mijarra, J.M., Morla, C., Barrón, E., Morales-Molino, C., García, S., 2010. Patterns of extinction and persistence of arctotertiary flora in Iberia during the quaternary. Rev. Paleobot. Palynol. 62, 416–426. https://doi.org/10.1016/j.revpalbo.2010.02.015.

Prentice, L.C., 1985. Pollen representation, source area, and basin size: towards a unified theory of pollen analysis. Quat. Res. 23, 76–86. https://doi.org/10.1016/0033-5894(85)90073-0.

Rasmussen, S.O., Seierstad, I.K., Andersen, K.K., Bigler, M., Dahl-Jensen, D., Johnsen, S.J., 2008. Synchronization of the NGRIP, GRIP, and GISP2 ice cores across MIS 2 and palaeoclimatic implications. Quat. Sci. Rev. 27, 18–28. https://doi.org/10.1016/j.quascirev.2007.01.016.

Reille, M., 1999. Pollen et spores d'Europe et d'Afrique du Nord, second ed. Laboratoire de Botanique Historique et Palynologie, Marseille.

Reimer, P.J., Bard, E., Bayliss, A., Beck, J.W., Blackwell, P.G., Bronk Ramsey, C., Buck, C.E., Cheng, H., Edwards, R.L., Friedrich, M., Grootes, P.M., Guilderson, T.P., Haflidason, H., Hajdas, I., Hatté, C., Heaton, T.J., Hoffmann, D.L., Hogg, A.G., Hughen, K.A., Kaiser, K.F., Kromer, B., Manning, S.W., Niu, M., Reimer, R.W., Richards, D.A., Scott, E.M., Southon, J.R., Staff, R.A., Turney, C.S.M., van der Plicht, J., 2013. Intcal13 and marine13 radiocarbon age calibration curves 0–50,000 years cal yr BP. Radiocarbon 55, 1869–1887. https://doi.org/10.2458/azu_js_rc.55.16947.

Renault-Miskovsky, J., Girard, M., Trouin, M., 1976. Observations de quelques pollens d'Oléacées au microscope électronique à balayage. Bull. AFEQ 2, 71–86.

Reyes, O., Casal, M., 1998. Are the dominant species in N.W. Spain fire-prone? In: Trabaud, L. (Ed.), Fire Management and Landscape Ecology. Fairfield, Washington, pp. 177–188.

Rivas-Martínez, S., 2007. Mapa de series, geoseries y geopermaseries de vegetación de España. Memoria del mapa de la vegetación potencial de España, parte I. Itinera Geobot. 17, 5–435.

Roberts, C.N., Stevenson, T., Davis, B., Cheddadi, R., Brewster, S., Rosen, A., 2004. Holocene climate, environment and cultural change in the circum-Mediterranean region. In: Battarbee, R.W., Gasse, F., Stickley, C.E. (Eds.), Past Climate Variability through Europe and Africa. Springer, Dordrecht, pp. 343–362.

Rodrigo-Gámiz, M., Martínez-Ruiz, F., Jiménez-Espejo, F.J., Gallego-Torres, D., Nieto-Moreno, V., Romero, O., Ariztegui, D., 2011. Impact of climate variability in the western Mediterranean during the last 20,000 years: oceanic and atmospheric responses. Quat. Sci. Rev. 30 https://doi.org/10.1016/j.quascirev.2011.05.011, 2018–2034.

Rubiales, J.M., García-Amorena, I., Génova, M., Gómez-Manzaneque, F., Morla, C., 2007. The Holocene history of highland pine forests in a submediterranean mountain: the case of Gredos mountain range (Iberian Central range, Spain). Quat. Sci. Rev. 26, 1759–1770. https://doi.org/10.1016/j.quascirev.2007.04.013.

Rubiales, J.M., García-Amorena, I., Hernández, L., Génova, M., Martínez, F., Gómez-Manzaneque, F., Morla, C., 2010. Late quaternary dynamics of pinewoods in the iberian mountains. Rev. Palaeobot. Palynol. 162, 476–491. https://doi.org/10.1016/j.revpalbo.2009.11.008.

Ruiz-Alonso, M., Pérez-Díaz, S., López-Sáez, J.A., 2019. From glacial refugia to the current landscape configuration: permanence, expansión and forest management of Fagus sylvatica L. in the Western Pyrenean Region (Northern Iberian Peninsula). Veg. Hist. Archaeobotany 28, 481–496. https://doi.org/10.1007/s00334-018-0707-6.

Ryan, P.A., Blackford, J.J., 2010. Late Mesolithic environmental change at Black Heath, south Pennines, UK: a test of Mesolithic woodland management models using pollen, charcoal and non-pollen palynomorphs data. Veg. Hist. Archaeobotany 19, 545–558. https://doi.org/10.1007/s00334-010-0263-1.

Sadori, L., 2018. The Lateglacial and Holocene vegetation and climate history of Lago di Mezzano (central Italy). Quat. Sci. Rev. 202, 30–44. https://doi.org/10.1016/j.quascirev.2018.09.004.

Sangüesa-Barreda, G., Camarero, J.J., Sánchez-Salguero, R., Gutiérrez, E., Linares, J.C., Génova, M., Ribas, M., Tíscar, P.A., López-Sáez, J.A., 2019. Droughts and climate warming desynchronize Black pine growth across the Mediterranean Basin. Sci. Total Environ. 697, 133989. https://doi.org/10.1016/j.scitotenv.2019.133989.

Sardinero, S., 2004. Flora y vegetación del macizo Occidental de la Sierra de Gredos (Sistema Central, España). Guineana 10, 1–474.

Schönswetter, P., Stehlik, I., Holderegger, R., Tribsch, A., 2005. Molecular evidence from glacial refugia of mountain plants in the European Alps. Mol. Ecol. 14, 3547–3555. https://doi.org/10.1111/j.1365-294X.2005.02683.x.

Schröder, T., van't Hoff, J., López-Sáez, J.A., Viehberg, F., Melles, M., Reicherter, K.,

2018. Holocene climatic and environmental evolution on the southwestern Iberian Peninsula: a high-resolution multi-proxy study from Lake Medina (Cádiz, SW Spain). Quat. Sci. Rev. 198, 208–225. https://doi.org/10.1016/j.quascirev.2018.08.030.

Sugita, S., 1994. Pollen representation of vegetation in quaternary sediments: theory and method in patchy vegetation. J. Ecol. 82, 881–897. https://doi.org/10.2307/2261452.

Taberlet, P., Fumagalli, L., Wust-Saucy, A., Cosson, J., 1998. Comparative phylogeography and postglacial colonization routes in Europe. Mol. Ecol. 8, 1923–1934. https://doi.org/10.1046/j.1365-294x.1998.00289.x.

Tarroso, P., Carrión, J.S., Dorado, M., Queiroz, P., Santos, L., Valdeolmillos, A., Alves, P.C., Brito, J.C., Cheddadi, R., 2016. Spatial climate dynamics in the Iberian Peninsula since 15 000 years. Clim. Past 12, 1137–1149. https://doi.org/10.5194/cp-12-1137-2016.

Telford, R.J., Birks, H.J.B., 2005. The secret assumption of transfer functions: problems with spatial autocorrelation in evaluating model performance. Quat. Sci. Rev. 24, 2173–2179. https://doi.org/10.1016/j.quascirev.2005.05.001.

Tomasso, A., Cheung, C.F., Fornage-Bontemps, S., Langlais, M., Naudinot, N., 2018. Winter is coming: what happened in western European mountains between 12.9 and 12.6 ka cal. BP (beginning of the GS1). Quat. Int. 465, 210–221. https://doi.org/10.1016/j.quaint.2017.12.020.

Turu, V., Carrasco, R.M., Pedraza, J., Ros, X., Ruiz-Zapata, B., Soriano-López, J.M., Mur-Cacuho, E., Pélachs-Mañosa, A., Muñoz-Martín, A., Sánchez, J., Echeverria-Moreno, A., 2018. Late glacial and post-glacial deposits of the Navamuño peatbog (Iberian Central System): chronology and paleoenvironmental implications. Quat. Int. 470, 82–95. https://doi.org/10.1016/j.quaint.2017.08.018.

Ubera, J.L., Galán, C., Guerrero, F.H., 1988. Palynological study of the genus Plantago in the iberian peninsula. Grana 27, 1–15. https://doi.org/10.1080/00173138809427728.

van Geel, B., 1978. A palaeoecological study of Holocene peat bog sections in Germany and The Netherlands, based on the analysis of pollen, spores and macroand microscopic remains of fungi, algae, cormophytes and animals. Rev. Palaeobot. Palynol. 25, 1–120. https://doi.org/10.1016/0034-6667(78)90040-4.

van Geel, B., 2001. Non-pollen palynomorphs. In: Smol, J.P., Birks, H.J.B., Last, W.M. (Eds.), Tracking Environmental Change Using Lake Sediments, vol. 3. Kluwer, Dordrecht, pp. 99–119. Terrestrial, algal, and siliceous indicators.

van Geel, B., Hallewas, D.P., Pals, J.P., 1983. A late Holocene deposit under the westfriese zeedijk near enkhuizen (prov. Of noord-holland, The Netherlands): palaeoecological and archaeological aspects. Rev. Palaeobot. Palynol. 38, 269–335. https://doi.org/10.1016/0034-6667(83)90026-X.

van der Knaap, W.O., van Leeuwen, J.F.N., 1994. Holocene vegetation, human impact, and climatic change in Serra da Estrela. Portugal. Diss. Bot. 234, 497–535. https://doi.org/10.7892/boris.81078.

van der Knaap, W.O., van Leeuwen, J.F.N., 1995. Holocene vegetation and degradation as responses to climatic change and human activity in the Serra da Estrela. Portugal. Rev. Palaeobot. Palynol. 89, 153–211. https://doi.org/10.1016/0034-6667(95)00048-0.

van der Knaap, W.O., van Leeuwen, J.F.N., 1997. Late Glacial and early Holocene vegetation sucession, altitudinal vegetation zonation, and climatic change in the Serra da Estrela. Portugal. Rev. Palaeobot. Palynol. 97, 239–285. https://doi.org/10.1016/S0034-6667(97)00008-0.

van der Knaap, W.O., Leeuwen, J.F.N., Finsinger, W., Gobet, E., Pini, R., Schweizer, A., Valsecchi, V., Ammann, B., 2005. Migration and population expansion of Abies, Fagus, Picea, and Quercus since 15000 years in and across the Alps, based on pollen percentage threshold values. Quat. Sci. Rev. 24, 645–680. https://doi.org/10.1016/j.quascirev.2004.06.013.

van der Plicht, J., van Geel, B., Bohncke, S.J.P., Bos, J.A.A., Blaauw, M., Speranza, A.O.M., Muscheler, R., Björck, S., 2004. The Preboreal climate reversal and a subsequent solar-forced climate shift. J. Quat. Sci. 19, 263–269. https://doi.org/10.1002/jqs.835.

Vannière, B., Colombaroli, D., Chapron, E., Leroux, A., Tinner, W., Magny, M., 2008. Climate versus human-driven fire regimes in Mediterranean landscapes: the Holocene record of Lago dell'Accesa (Tuscany, Italy). Quat. Sci. Rev. 27, 1181–1196. https://doi.org/10.1016/j.quascirev.2008.02.011.

Vannière, B., Colombaroli, D., Roberts, N., 2010. A fire paradox around the Mediterranean. PAGES Newlett. 18, 63–65. https://doi.org/10.22498/pages.18.2.63.

Vannière, B., Power, M.J., Roberts, N., Tinner, W., Carrión, J.S., Magny, M., Bartlein, P., Colombaroli, D., Daniau, A.L., Finsinger, W., Gil-Romera, G., Kaltenrieder, P., Magri, D., Pini, R., Sadori, L., Turner, R., Valsechi, V., Vescovi, E., 2011. Circum-Mediterranean fire activity and climate changes during the mid-Holocene environmental transition (8500-2500 cal. BP). Holocene 21, 53–73. https://doi.org/10.1177/0959683610384164.

Vargas, P., 2003. Molecular evidence for multiple diversification patterns of alpine plants in Mediterranean Europe. Taxon 52, 463–476. https://doi.org/10.2307/3647333.

Vargas, P., García, B., 2008. Plant endemics to Sierra de Gredos (central Spain): taxonomic, distributional, and evolutionary aspects. Anales Jard. Bot. Madrid 65, 353–366. https://doi.org/10.3989/ajbm.2008.v65.i2.298.

Viedma, O., 2008. The influence of topography and fire in controlling landscape composition and structure in Sierra de Gredos (Central Spain). Landsc. Ecol. 23, 657–672. https://doi.org/10.1007/s10980-008-9228-5.

Watts, W.A., Allen, J.R.M., Huntley, B., 1996. Vegetation history and palaeoclimate of the last glacial period at Lago Grande di Monticchio, southern Italy. Quat. Sci. Rev. 15, 133–153. https://doi.org/10.1016/0277-3791(95)00093-3.

Wei, D., González-Sampériz, P., Gil-Romera, G., Harrison, S.P., Prentice, I.C., 2019. Climate changes in interior semi-arid Spain from the last interglacial to the late Holocene. Clim. Past Discuss. https://doi.org/10.5194/cp-2019-16.

Yu, Z., Eicher, U., 2001. Three amphi-Atlantic century-scale cold events during the Bølling-Allerød warm period. Géogr. Phys. Quaternaire 55, 171–179. https://doi.org/10.7202/008301ar.

Zumbrunnen, T., Bugmann, H., Conedera, M., Burgi, M., 2009. Linking forest fire regimes and climate - a historical analysis in a dry inner alpine valley. Ecosystems 12, 73–86. https://doi.org/10.1007/s10021-008-9207-3.